Analysis of Nevada Seismicity Using Improved Locations, Focal Mechanisms and Stress Drops: Collaborative Research between U.C. San Diego and U. Nevada Reno

USGS Earthquake Research Program Award # G16AP00035/36

Final Technical Report: November 30, 2017

Dr. Peter Shearer
Scripps Institution of Oceanography
U.C. San Diego
San Diego, CA 92093-0225
858-534-2260 (office), 858-534-5332 (fax)
pshearer@ucsd.edu

Dr. Rachel Abercrombie, Temporary Research Faculty
U. Nevada Reno/Nevada Seismological Laboratory
1664 N. Virginia St. MS0174
775-784-1396 (office), 775-682-8427 (fax)
rea@bu.edu

Dr. Kenneth Smith
U. Nevada Reno/Nevada Seismological Laboratory
1664 N. Virginia St. MS0174
Reno, NV 89557-0174
775-784-1396 (office), 775-682-8427 (fax)
ken@seismo.unr.edu

Award Dates: March 1, 2016 – August 30, 2017

Graduate Students:

Daniel Trugman (UC San Diego Ph.D., recently awarded)
U.C. San Diego
San Diego, CA 92093

Dr. Christine Ruhl (Ph.D. UNR 2016)
Post-Doctoral Fellow
U.C. Berkeley Seismology Lab
Berkeley, California

Rachel Hatch (UNR Ph.D. Candidate)
University of Nevada Reno
Reno, NV 89557

Abstract

This collaborative project between the University of California, San Diego (UCSD) and the University of Nevada, Reno (UNR), applied automated processing methods to seismic data recorded by the Nevada Regional Network and available temporary networks. These methods provide a practical way to systematically examine the large seismic databases collected from permanent and portable networks in Nevada. We performed waveform cross-correlation for similar event cluster identification and high-precision earthquake relocation, focal mechanism analyses, and comprehensive spectral computations for earthquake stress drops and attenuation studies. Our focus during this initial phase of funding was on several swarms and regional earthquake sequences, for which we obtained temporal and structural details, source parameter estimates, and inferences regarding the stress field. Our results, described in a number of papers and conference presentations, have contributed to an integrated strategy for understanding the details and attributes of Nevada seismicity associated with Walker Lane deformation as well as the driving mechanisms of earthquake swarms. Given additional funding support, we plan to continue this work by performing detailed studies of additional areas of persistent seismicity with the goal of gaining an integrated view of Nevada seismicity, tectonics, and seismic hazard.

1.0 Introduction

Nevada is second only to California of the lower-48 states in long-term seismic activity. An ~M6 earthquake occurs in the Nevada region (the Nevada network covers Nevada and areas of eastern California) about every three years; there were three M ~7 events in the 1900s in state. NSL processes an average of ~1.7 M ≥ 3 events per week and locates between 15,000 and 19,000 events per year with its modernized network (i.e., support through the ARRA, the USGS and other agencies). These activity rates far exceed all WUS networks except for California. The NSL currently operates ~120 stations, and there are ~100,000 M ≥ 1 earthquakes in the NSL waveform database since 1984.

The aim of our work is to develop and begin applying state of the art processing methods to this large database, so as to improve our understanding of ongoing active deformation in Nevada, and the seismic hazard that it represents. In California, high-precision event relocations (e.g., Shearer et al., 2006), Waldhauser, 2001), combined with calculation of focal mechanisms, stress inversion, and inversion for regional attenuation and source parameters (Shearer and Hauksson, 2006) have vastly increased our understanding over the last decade. The long-term goal of our collaboration is to obtain the same level of understanding of earthquakes and seismic hazard in Nevada. This is clearly an ambitious and multi-year endeavor, and here we describe the significant steps we have taken towards this longer-term goal.

Before new methods can be applied to such a large regional database of earthquakes, they must be tested, and adapted, using smaller subsets. As such, we have focused on applying different approaches to specific sequences of earthquakes, chosen either as good candidates for testing, or because they are of significant public interest. These include two older sequences, and three that happened within the duration of this award.

1. Spanish Springs: ideal sequence to test new relocation methods, felt throughout Reno
2. Mogul Sequence: felt throughout Reno area, relocation and source parameters
3. Nine Mile Ranch 2016-2017: 3 M ~5.5 event; widely felt, local damage, relocations
4. Sheldon 2014-2016: strongly felt, relocations and source parameters
5. Truckee 2017: strongly felt, near urban areas, relocations and source parameters

We begin with an introduction to Nevada seismicity and deformation, a description of methods developed and applied and then describe our work on each sequence in turn. We focus on the methods developed as applied to the details of each sequence. We finish by describing the initial

efforts carried out for a number of other sequences, including initial relocation of 15 years of seismicity in the northern and the eastern Sierra region, between Mammoth Lakes and the Reno area, and an analysis of the stress field in the vicinity of the Nevada National Security Site (NNSS).

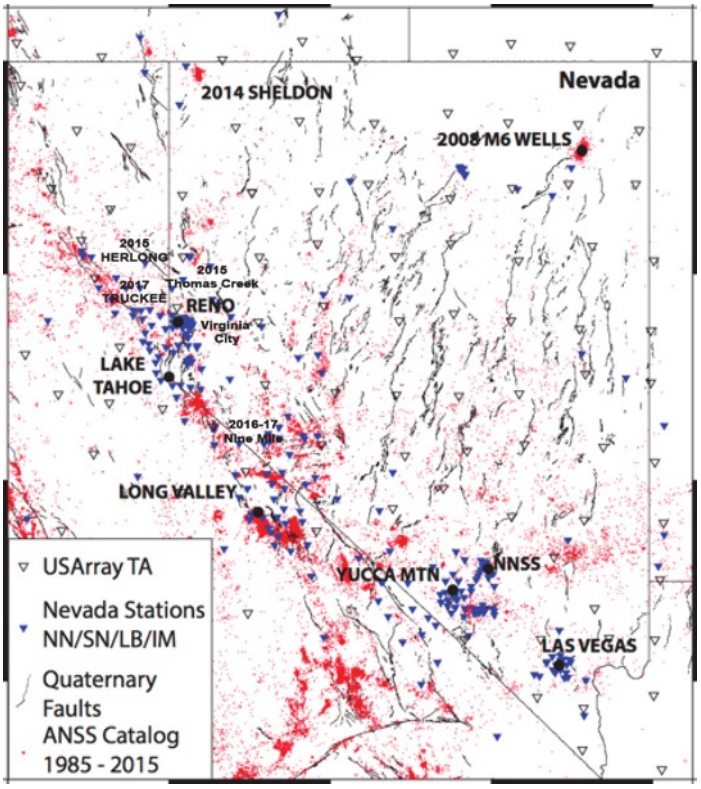

Figure 1. Seismicity features of Nevada and surrounding areas monitored by the NSL, as from the ANSS catalog [1984-2014 (red dots). NNSS: Nevada National Security Site. The gray lines are for the USGS Quaternary faults database (U.S. Geological Survey, Nevada Bureau of Mines and Geology, and California Geological Survey 2008, Quaternary fault and fold database for the United States). The Walker Lane bounds the eastern Sierra and extends about 100 km into the western Basin and Range of Nevada.

The majority of the regional seismicity occurs within the Walker Lane of western Nevada and eastern California (Figure 1) and reflects ~20-25% of the relative Pacific-North America strain budget determined from geodetic studies east of the Sierra Nevada (Argus and Gordon, 1991; Faulds and Henry, 2008). Consequently, these are the regions where the monitoring network is most dense and most sensitive and where earthquake clusters can best be defined. Additionally, NSL has operated a dense network in the southern Nevada area, beginning with the Yucca Mountain Project 1992 and more recently in the vicinity of NNSS. Deformation within the Walker Lane is accommodated through a complex distribution of NW-striking dextral and secondary NE-striking sinistral strike-slip systems and primarily down-to-the-east normal faulting along the eastern Sierra and other normal systems. The NW-striking dextral faults of the southern, central and northern Walker Lane directly accommodate plate-boundary shear (e.g., Faulds et al., 2005). Range-front normal faulting and structural transition zones along left-stepping normal faults in the northeastern Sierra, and a complex array of other fault systems also act to accommodate regional strain, all contributing to the seismic hazard in the populated areas of Reno-Carson City-Truckee and Lake Tahoe region. Instrumentally-recorded seismicity has generally not been observed on major range-bounding fault systems, but is instead generally concentrated at the ends of these faults (van Wormer and Ryall, 1980; Ichinose et al., 1998), in interpreted source zones not associated with mapped structures, and in clusters of seismicity distributed throughout the Walker Lane.

The largest historical events in Nevada have occurred on range-bounding normal faults of the Basin and Range, along the eastern Sierra and in the central Nevada seismic belt. Of particular importance and interest to the populated areas of the Reno-Carson City-Lake Tahoe region is the common occurrence of earthquake swarms, such as the extended 2008 Mogul sequence (Ruhl et al., 2016; Ruhl et al., 2017) that caused several million dollars in damage in urban Reno. Seismic

swarms are poorly understood; well-recorded sequences in Nevada, such as the Mogul sequence and others outlined below, provide an opportunity to investigate the physical characteristics and spatiotemporal evolution of these active sources.

The availability of high-quality digital seismic data and modern, low-cost data storage now make it possible to work with large data sets and to perform complex measurements on thousands to millions of waveforms. In addition, Shearer et al. (2006) developed a comprehensive analysis method for P-wave spectra, yielding over 60,000 stress-drop estimates for small earthquakes in southern California. This has been extended in this study to better quantify spectral EGF methods for source parameter estimates from P and S waveforms. Because individual event stress drops exhibit large scatter, analyses of large numbers of events are important for statistically establishing spatial and temporal variations in average stress drop and reducing the uncertainty in these measurements. However, to validate the approach it is important to compare the results with stress studies obtained using more traditional methods for specific regions in common. There is a wealth of data in Nevada for studies of source parameters in a transtensional tectonic environment.

2.0 Methods Applied in Analysis of Seismicity and Source Parameters

We applied a number of different analysis methods in our research, which, for reference, we introduce here. They are a combination of both existing techniques, and ones that we developed or modified during this award. We describe the newer techniques in more detail in the discussion of work on individual sequences where they were further developed and tested.

2.1 Earthquake Relocation using HypoDD

The USGS HypoDD relative relocation code (Waldhauser, 2001) was already in use in Nevada and had been used in an initial regional analysis by Ruhl et al. (2016). HypoDD input is also built directly from the Antelope Datascope database. This algorithm is now over 15 years old.

2.2 Earthquake Relocation using GrowClust, a Newly Developed Relocation Method

The GrowClust relocation algorithm (Trugman and Shearer, 2017) is an improved version of methods previously applied by the UCSD group under PI Shearer to perform waveform cross-correlation and event relocation of massive earthquake datasets in southern California and Hawaii. We developed and tested this algorithm using data from the Spanish Springs and Sheldon sequences, where GrowClust results are compared directly with HypoDD.

2.3 Focal Mechanism Determination using HASH

First motion P-wave short-period focal mechanisms are determined with the USGS software application HASH (Hardebeck and Shearer, 2002) and are used to supplement moment tensor solutions, in each sequence studied. HASH has the advantage of using multiple velocity models, configurable parameters for accepting a percentage of 'bad' polarities, and statistically derives a best-fitting set of mechanisms. HASH input is built directly from the NSL Antelope Datascope database for specified regions and has been adapted for routine network processing and USGS ComCat XML postings and local database updates.

2.4 Regional Moment Tensor Solutions using MTINV

Moment tensor solutions are derived from regional surface-wave fits to synthetics given a regional velocity model using the MTINV application (Ichinose, 2013). MTINV calculates synthetic seismograms for a given source receiver pair precluding the need to maintain libraries of Green's functions and moment tensors are calculated in real-near and/or reviewed within minutes of an event. NSL has integrated the capability within the MTINV package to access broadband data from the IRIS data center using IRIS web-based tools. In principle, MTINV be used for any global event where a reasonable 1-D model applies. Since 2011 NSL has compiled about 320 moment tensor

solutions during routine network operations, which are included in the studies below; MTINV results are consistently similar to moment tensor solutions developed by CISN and NEIC.

2.5 Stress Field Inversion using SATSI

We apply the stress inversion technique, SATSI, of Hardebeck and Michael (2006) to determine a best fitting stress field for regional data sets. Since most of Nevada is poorly monitored, often focal mechanisms are difficult to determine. The HASH application addresses some of these issues and the HASH derived focal mechanisms are used to model and local regional stress fields. The SATSI algorithm applies regularization to find the smoothest stress field that is consistent with the data and thus only retains variations that are well resolved.

2.6 Earthquake Stress Drops using P-wave Spectral Decomposition EGF Method

Shearer et al. (2006) developed a comprehensive analysis method for P-wave spectra, yielding over 60,000 stress-drop estimates for small earthquakes in southern California. This method, as modified and improved by Trugman and Shearer (2017b) is used to calculate stress drops for the 2012-2014 Spanish Springs sequence.

2.7 Earthquake Stress Drops using Newly Developed EGF Spectral Ratio Method

This method was developed over the course of this study, using the Mogul sequence in particular for testing and adaptation (Ruhl et al., 2017). Each event of interest (target event) is analyzed independently, and carefully selected EGFs are used to correct for the instrument, path, and site responses of the target event. A significant effort was undertaken to better understand uncertainties in stress drop estimates.

2.8 Source Directivity using STF Stretching Method

Abercrombie et al. (2017) demonstrated that for the best recorded earthquakes, the source time functions from the EGF analysis can be stacked by station to show azimuthal rupture geometry variations. Prieto et al. (2017) and Abercrombie et al. (in press) developed a stretching method introduced by Warren and Silver (2006) to quantify the azimuthal variation using the whole shape of the source time function. This approach is able to identify the fault plane, and so confirmed the fault structures implied from earthquake alignments in the Mogul sequences. It has also proved important in understanding the inter-event relationships of the 2017 Truckee, CA sequence.

3 Analysis of Nevada Seismicity

3.1 2012-2014 The Spanish Springs Swarm

This complicated swarm consisted of over 1600 earthquakes in the north Reno area, mainly during three relatively short bursts of activity. The most prominent increase in activity was associated with an M4.2 event on 8/27/2013 (mainshock). This earthquake was widely felt throughout the Reno area and caused minor damage to several URMs in Reno and on the UNR campus. Most of the locatable events in the swarm were identified by scanning the continuous waveforms where subtle P-wave arrivals, particularly on analog stations, would be difficult to recognize even, in our opinion, with matched filtering techniques. Catalog locations for this swarm show a typical ‘cloud’ of activity (see Figure 2), but are suggestive of a NE trending structure. Much better resolution has been achieved by reducing the scatter due to location errors. To achieve this, we have applied both the double-difference method (Waldhauser and Ellsworth, 2000) and the GrowClust method UCSD (Trugman and Shearer, 2017a).

3.1.1 Earthquake Relocations

The GrowClust relocation algorithm (Trugman and Shearer, 2017a) is an improved version of methods previously applied by the UCSD group under P. Shearer to perform waveform cross-

correlation and event relocation of massive earthquake datasets in southern California. As used here, estimates of absolute event locations are determined initially using HYPOINVERSE (Klein, 2002) with a datum correction to account for topographic relief (Ruhl et al., 2016). Average station residuals from these initial locations are applied in a subsequent HYPOINVERSE run for a final set of absolute location estimates and used as input to the GrowClust routine. Data is prepped for input to the GrowClust process by sub-setting all event data from the Antelope DataScope miniseed waveform database into SAC format under YEAR/EVID event directories. The SAC format files are converted to a multiplexed UCSD format for use with the UCSD developed cross-correlation routines, and ultimately the GrowClust routine. The process is straightforward and efficient, there are few parameters to adjust, and events are selected based on defined polygon searches over specific time periods to focus relocations to individual clusters or regions.

Waveform cross-correlations of P- and S-arrivals are performed for every event pair. With these cross-correlation results, we then relocated the events using GrowClust, an L1-norm method that integrates the cluster analysis and relocation steps into a single program (see Trugman and Shearer, 2017a, for details). About half of the earthquakes in the sequence were sufficiently correlated to be relocated. Surprisingly, even the M4.2 could be cross-correlated on many stations, despite its larger size and many clipped analog station records. The new locations are plotted in Figure 2 and show a remarkable level of detail.

In a separate analysis, we applied the hypoDD algorithm to these data, including computing cross-correlation differential times. The results are comparable to the GROWCLUST locations (see Figure 2), although not quite as sharply defined, giving us confidence that both methods are working well. There are many adjustable parameters in hypoDD, and it is possible that further improvements can be obtained (these results are shown in Trugman and Shearer, 2017a).

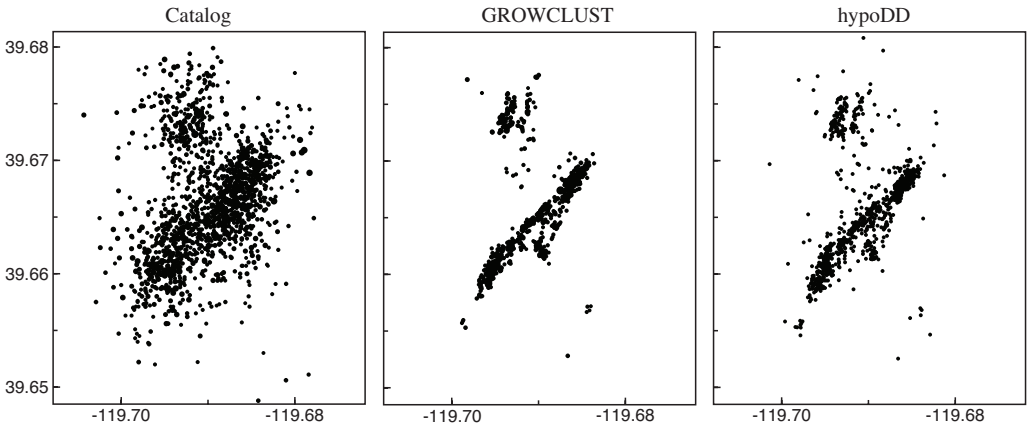

Figure 2. The Spanish Springs swarm, showing a comparison of the original catalog locations (left) and our new locations, computed using both GROWCLUST (middle) and hypoDD (right).

So far, we have noted the following: (1) we obtain the best locations when only differential times derived from waveform cross-correlation are used, i.e., no catalog picks are used, (2) the waveform cross-correlations computed using the UCSD algorithm produce somewhat sharper locations when used in hypoDD than those computed using various hypoDD 'ph2dt' parameters and a limited number of cross-correlation times. Cross-correlation times from the UCSD codes can be output in hypoDD format. We continue to compare the locations obtained with the different methods and approaches in an effort to better understand performance improvements in both algorithms.

Most of the events are located on a narrow NE trending fault about 1.5 km long. The fault appears nearly vertical (see Trugman and Shearer, 2017a). An off-fault cluster of events in 2012 is most likely on a separate structure; there are two sub-clusters of small events north of the main

event. The most intriguing features are associated with the Mw4.2 mainshock. There was a well-defined 6-day long foreshock sequence, during which the activity migrated ~300 m northeastward along the primary fault toward the eventual mainshock hypocenter. These observations show that integrating high-quality location codes with near real-time routine processing can provide important information than can be translated directly to the emergency managers and the public. NSL conducted regular press conferences with local emergency managers emphasizing the risks to the local community, prior to the main event (a similar process was conducted prior to the 2008 Mogul mainshock and during the 2014 Virginia City sequence).

3.1.2 Focal Mechanisms

To further analyze this sequence, focal mechanisms were computed using the USGS HASH algorithm. As expected, only a small fraction of events yielded reliable mechanisms (see Figure 3), yet these are sufficient to define fundamental features of the sequence. The main fault trace, including the mainshock, is defined by left-lateral strike-slip events. However, activity near the ends of the fault is more complex and includes some normal-faulting earthquakes. The separate cluster to the north includes at least one oblique faulting event (Figure 3).

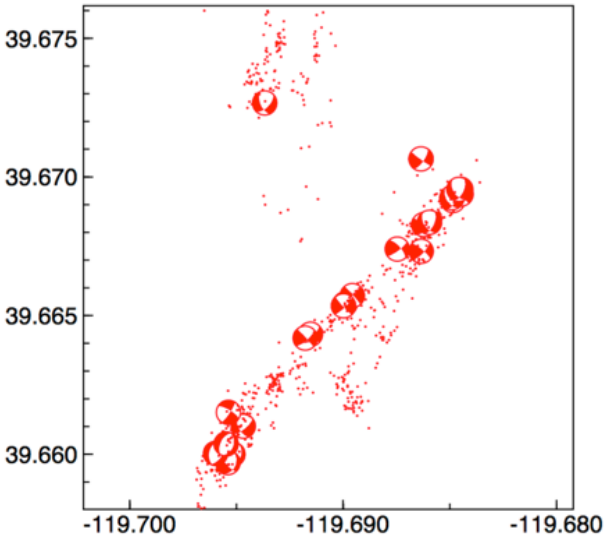

Figure 3. Short period focal mechanisms for the Spanish Springs sequence. A moment tensor solution was generated by NSL for the Mw 4.2 mainshock as part of routine analysis of M 3.5+ earthquakes in the Nevada region.

3.1.3 Stress Drop Analysis

Next, we computed P-wave spectra for these events and analyzed them using a new approach based on the iterative stacking procedure of *Shearer et al.* (2006), which solves for source, path, and station correction terms, and then solves for a best-fitting empirical Green's function (EGF) that best explains the changes in the spectral shapes with increasing moment. We then computed corner frequencies and estimate stress drops, assuming the Madariaga (1976) model. Because of the small size of most of the Spanish Swarm earthquakes, reliable results could only be obtained for a fraction of events. Stress drops range from 1 to 100 MPa. An advantage of this new approach compared to the original Shearer et al. (2006) algorithm is that we obtain formal uncertainty estimates. These should be considered preliminary results and the absolute values of stress drop are highly model dependent. However, the relative stress drops between different events are more robust. The Mw 4.2 mainshock has an above-average stress drop compared to the rest of the sequence. S-wave EGF spectral stacking stress drop comparisons have not yet been computed.

3.1.4 Sequence Summary

These results for the Spanish Springs swarm demonstrate the value of our collaboration by

revealing a much more detailed picture of the evolution of this sequence. We have integrated the UCSD location algorithms with NSL's Antelope database system for efficient processing and ease of comparison of location methods; file format conversions required by the UCSD approach have not been overly time consuming and are now very efficient. The UCSD GrowClust suite of relocation codes require directories of individual events, with all associated and/or defining phases, based on EVIDs. For conversion of several 1000 events this can be done fairly quickly, conducting relocations over wide regions with tens of thousands of events can require more than a day for the format conversions. This process has improved during the course of this study (the process is described above under "GrowClust", Section 2.2). We go into some detail in the analysis of the Spanish Springs sequence, but is basically the process applied to other sequences and regional relocations below. Additionally, earthquake stress drop estimation and directivity methods that have been developed during this study are noted below. GrowClust is now run routinely at UNR during local periods of increased seismicity, improving catalog locations and the understanding of the seismotectonics of ongoing activity.

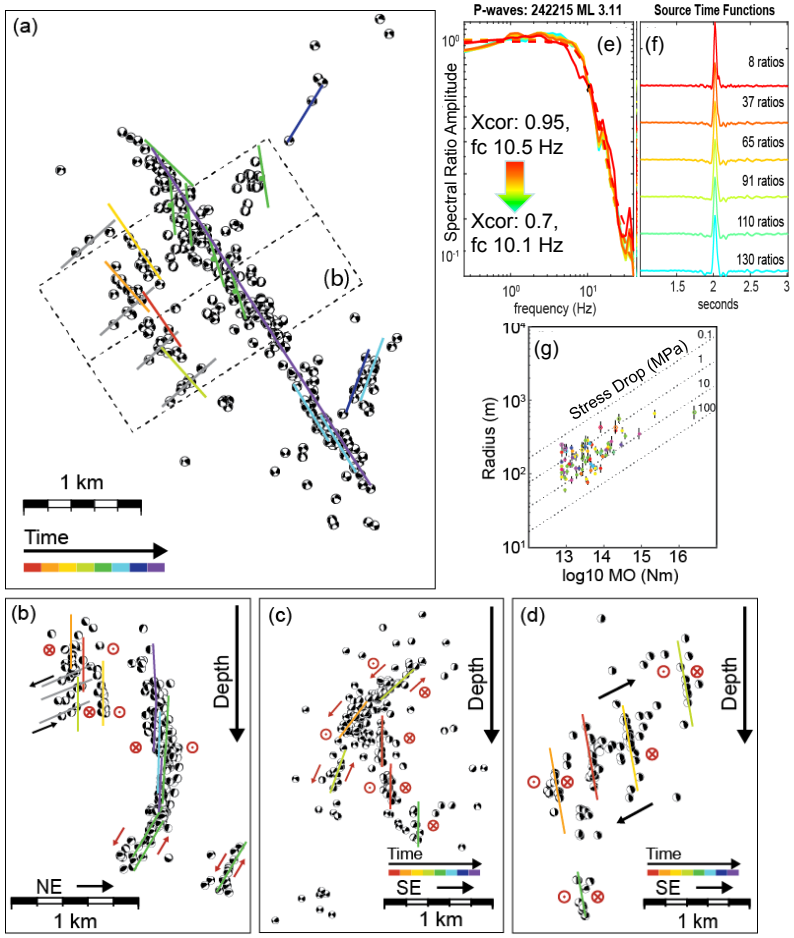

Figure 4. Localized analysis of the 2008 Mogul sequence. (a), (b), (c), and (d) show the relocated earthquakes with focal mechanisms in map view and cross section. The structure features are indicated by lines and colors showing time progression of the sequence (e) and (f) show example spectral ratios and source time functions from stacking only highly correlated (Xcor) EGF events. (g) shows calculated stress drops for P waves.

3.2 The 2008 Mogul, West Urban Reno, Earthquake Sequence

An energetic, shallow (≤ 6 km) earthquake swarm produced over 15,000 detected events over several months in 2008, including hundreds of small felt events in the Mogul and Somersett communities of west Reno. Ruhl et al. (2016) provides an extensive analysis of the Mogul earthquake sequence. After two months of swarm-like earthquakes, seismicity rates accelerated, culminating in the largest event of the sequence, an M_w 4.9. The largest event was proceeded for

two-months of bursts of apparently independent microseismicity ultimately forming distinct structures within the sequence. Although very shallow, the northwest-striking, right-lateral strike-slip mainshock slip area does not conform to locally mapped faults (Smith et al., 2008). Rapid temporary instrument deployment provided high-resolution coverage for a detailed analysis of the swarm's behavior and complex faulting geometry (Figure 4a).

3.2.1 Mogul Sequence Earthquake Relocations

We relocated 7549 earthquakes, using hypoDD in this case, and calculated a complementary set of 1100 focal mechanisms with HASH to understand the timing and interaction of active structures. Detailed relocations and visual analysis (Ruhl et al., 2016) indicate an internally clustered sequence in which foreshock seismicity evolved on multiple well-resolved structures that generally surround the eventual mainshock fault rupture (Figure 4). Internal clusters were objectively isolated using an adaption of the nearest-neighbor method of Zaliapin and Ben-Zion (2013a, 2013b) to address local sequences. Prior to the M_w 4.9 mainshock, the seismicity is largely comprised of individual and independent mainshock-aftershock sequences occurring within diffuse background seismicity that may have been triggered by fluid flow or potentially aseismic deformation. The relocated seismicity defines a fault-fracture mesh and detailed structure from approximately 2–6 km depth on a previously unknown fault. This could be an evolving, insipient source zone that should perhaps be considered in assessing the local seismic hazard.

3.2.2 Stress Drop Analysis

To investigate stress drop, we worked on extending the approach of Abercrombie et al. (2017). Each event of interest (target event) is analyzed independently, and carefully selected EGFs are used to correct for the instrument, path, and site responses of the target event, thus isolating its source spectra. Potential EGFs considered are all events within 1-2.5M units smaller than the target. For EGF selection in detailed analysis of sequences, the hypocentral search radii follow the Wells and Coppersmith (1994) relationship between magnitude and rupture area, but a minimum hypocentral search distance of 0.5 km is set with respect to the target. Following Ruhl et al. (2017), for each target-EGF waveform a time window is selected for P- and S-wave arrivals, based on the magnitude of the target event, and the assumption of constant stress drop.

To date we have estimated source parameters for 148 earthquakes in the Mogul sequence using both P- and S-wave EGF-derived spectral ratios. High-quality EGFs are chosen by testing earthquakes that are within one estimated fault length to each target event, and the spectral ratios and source time functions are stacked to improve stability (Figure 4). We quantify the uncertainties from fitting and data quality, and find variations within the sequence greater than the error range of each individual estimate. There is no clear stress drop dependence on location, timing, depth, seismic moment, or mechanism type, however, there are more complex spatiotemporal patterns observed along the mainshock fault plane. Average stress drops for this shallow swarm are similar to previous studies of deeper events. This implies that other shallow, fluid-driven earthquakes (e.g., induced seismicity) should not be expected to have relatively low stress drops and lower "local" ground motions (*Ruhl et al.,* 2017).

3.2.3 Source Directivity

In addition, for the best-recorded earthquakes, we used stacks-by-station of the source time functions from the EGF analysis to investigate azimuthal variations related to fault geometry and rupture directivity. Preliminary orientation measurements often coincide with earthquake alignments, confirming the existence of complex fault structures interpreted from statistical clustering and focal mechanisms. This work is ongoing, and will be presented at the 2017 Fall AGU Meeting.

3.3 2017 Sequence North of Truckee, CA; Mw 3.65 and Mw 3.85

The Truckee 2017 sequence includes 142 events (as of Oct. 7th, 2017), and is confined to fairly shallow depths (5-6 km). The sequence began with a M_w 3.65 foreshock, with three smaller foreshocks occurring in the following minutes; 7 minutes after the initial foreshock, the M_w 3.85 mainshock occurred (Figure 5). Initial aftershocks persisted for ~4 days in late June, producing 52 events, including 3 M3 and 8 M2 events. After this period of time, the sequence started to decline to a rate of ~1 event/day over the next 3 months. We confine our analysis to the ~4-day period of elevated aftershock activity.

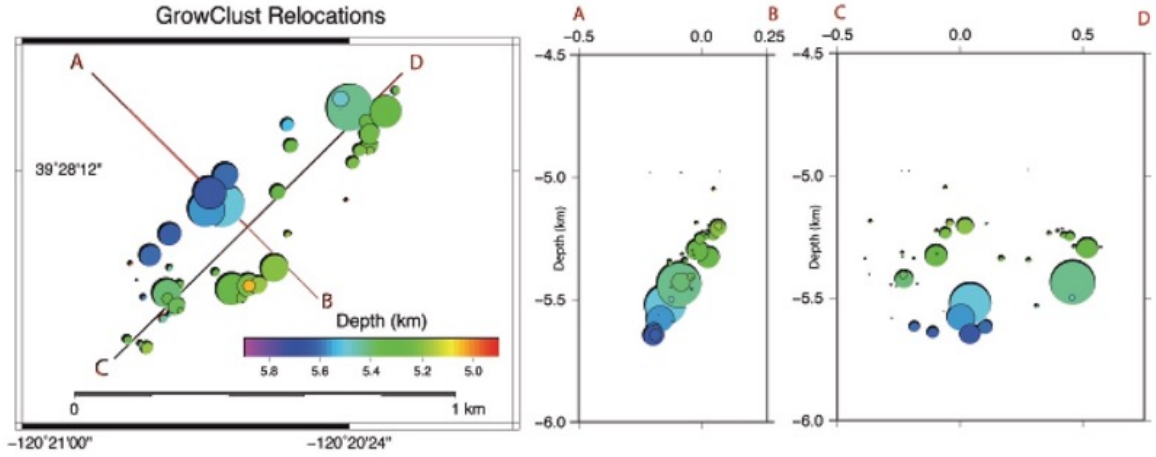

Figure 5. Relocations of 2017 Truckee sequence. Fault dips at a high-angle, ~70 degrees, to the NW and extends in a NE-SW orientation for ~1 km.

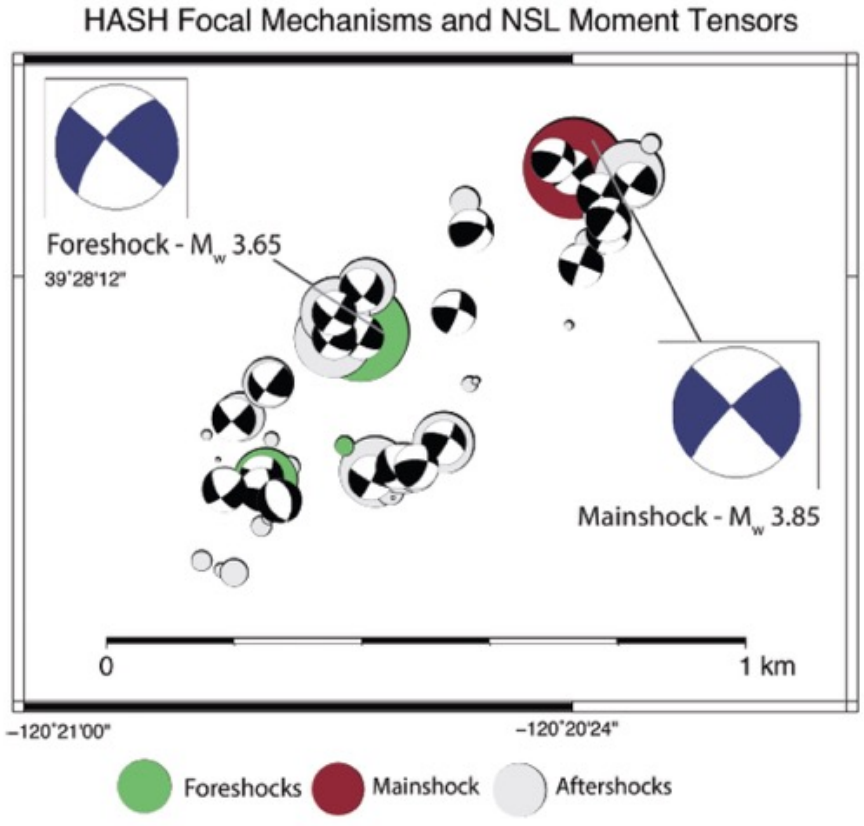

Figure 6. Relocations, moment tensor solutions for the two largest events, and HASH short-period mechanisms for the Truckee sequence, map view.

3.3.1 Truckee Sequence Relocations

The GrowClust location error averages ~30 m; maximum horizontal error is 21 m and maximum vertical error 169 m. As shown in Figure 5, the relocations show a planar generally elliptical structure about 0.8-1.0 km long, striking ~N45E and dipping 70-80° NW. There are no obvious sub-structures or alternate geometries in the relocation set; all activity is confined to a single well-defined NE striking fault plane that agrees with the moment tensor and HASH short period focal mechanism for the largest event (Figure 6). The sequence began with an Mw 3.65 foreshock (Origin Time: October 7, 2917; 02:02:01 PDT) located at depth near the central portion of the sequence. Two smaller foreshocks occur SW of the initial foreshock at the SW extent of the sequence. The Mw 3.85 mainshock (Origin Time: October 7, 2917; 02:09:21 PDT) locates at the far NE end of the of the sequence. Aftershocks outline a region of low seismicity; the aftershocks of larger earthquakes are typically observed to cluster around the regions of large slip (Ross et al., 2017 and references therein).

3.3.2 Truckee Sequence Stress Drop Analysis

Using the spectral EGF method, the source parameters for 9 events out of 11 potential target events (M_L 2-4.1) were estimated, with stress drops ranging from 0.4 to 14 MPa and average stress drops of 3 MPa and 5 MPa for P and S waves, respectively. Spatially, lower stress-drop events outline the rupture zone of the two largest events (interpreted from the relocations); the large foreshock and mainshock, have the highest stress drop (average P and S values) of 9.2 MPa and 9.0 MPa, respectively. Temporally, large events, occurring early in the sequence, have higher stress drops relative to the aftershocks in the sequence.

Eight of the 9 events where stress drops were calculated display good fits with a simple circular rupture model (Boatwright 1980), while only the mainshock shows variation in the source time function, interpreted as evidence of a more complex rupture. Using these stress-drop values and the circular rupture model, we calculate rupture radii of 0.37 (+0.06/-0.04) km and 0.30 (+0.04/-0.03) km for the mainshock and foreshock. Errors reflect 5% variance of the corner frequency pick. When combined, the total area of both ruptures is 0.71 km^2 (+0.23/-0.14 km^2).

3.3.3 Truckee Sequence Source Directivity

Preliminary results for the initial stack by station analysis show a narrower source time pulse between azimuth ~0-50° for the Mw 3.65 foreshock, as well as a narrower pulse width between ~160-360° for the Mw 3.85 main event. This first-order observation suggests possible components of directivity between N to NE azimuths for the foreshock, and between S to SE for the mainshock. After applying the stretching method our results are much more definitive and show clear directivity for both events. Best fit results for the foreshock and mainshock indicate components of unilateral rupture along the fault plane, and in opposite directions (Figures 7 and 8) for the two largest events. Unilateral directivity results show RMS values of 0.032 and 0.019 for both the foreshock and the mainshock, respectively. Bilateral rupture RMS results are higher, at values of 0.046 and 0.040. Asymmetrical 2:1 rupture results are indistinguishable from pure unilateral rupture and produce the same best fit direction, dip and rupture velocity, so we cannot discard the possibility of a bilateral rupture component to both events. More specifically, our results show directivity to ~N50E for the Mw 3.65 foreshock near the central/southwest end of the fault, and directivity to ~S40W for the Mw 3.85 mainshock, at the northeast extent of the sequence, essentially bracketing more than half of the ~1 km rupture area. RMS differences are marginal between the unilateral and bilateral rupture tests; this may be due to our lack of station coverage to the west. Nevertheless, best fits for directivity directions for both events are consistent with the NE-SW striking fault plane form the moment tensor solutions and event relocations.

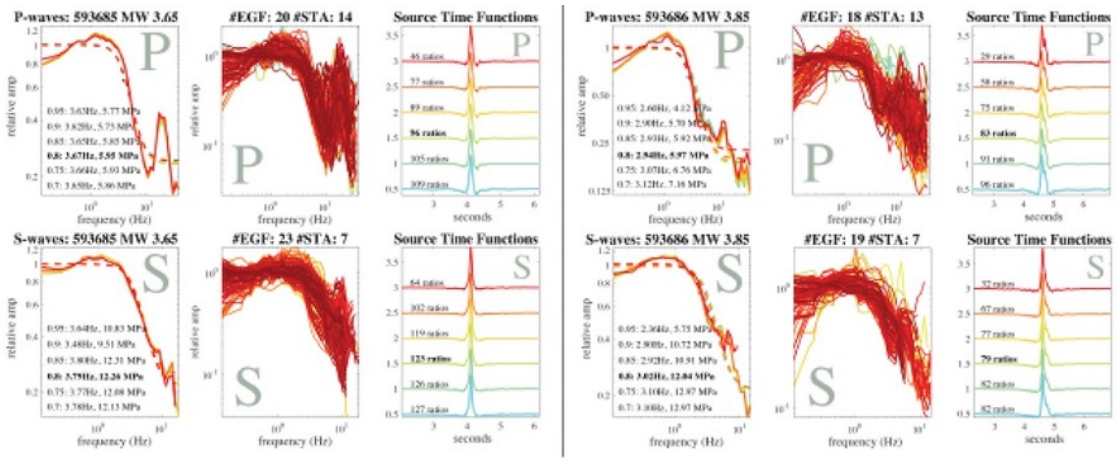

Figure 7. Illustrates stacking and fitting method for determining Source Time Functions (STF) for the two largest events based on different cross-correlation criteria.

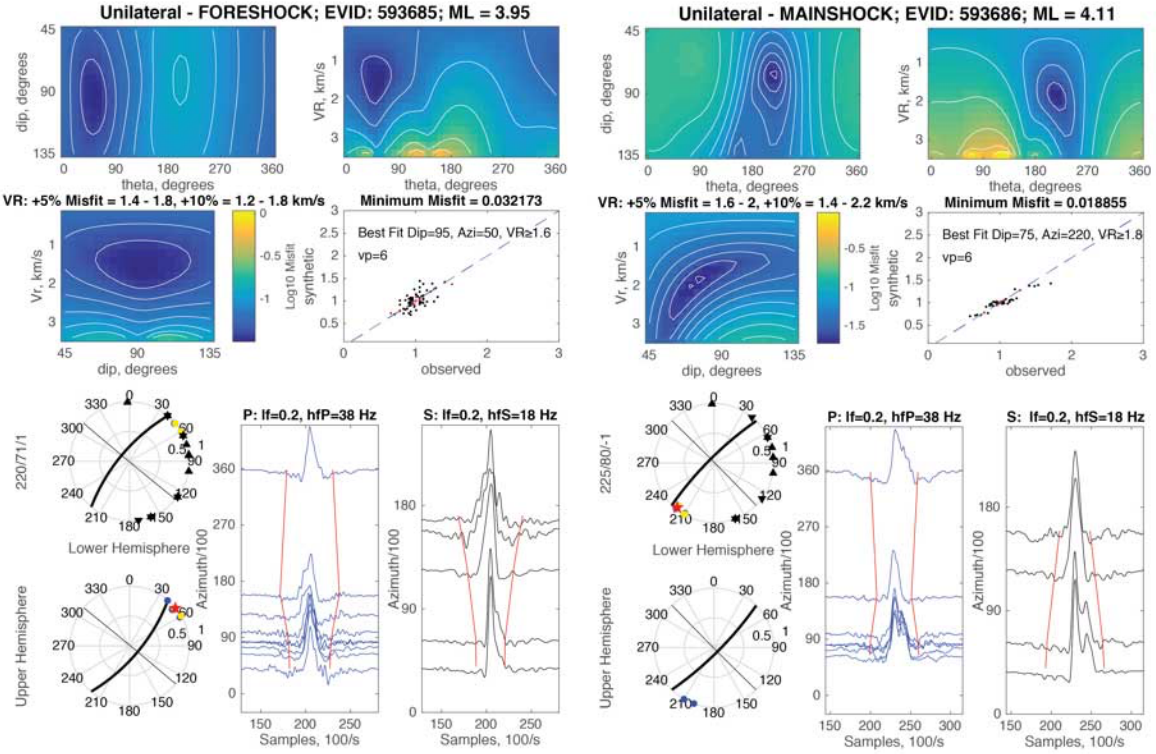

Figure 8. Unilateral rupture directivity analysis of the two large events of the Truckee sequence showing the preferred rupture direction applying STF stretching technique (Abercrombie et al., in press).

3.4 2014-2016 Northwest Nevada/Sheldon Sequence; 300+ M3 Events

Between July 2014 and November 2017, 8,089 events have been located in the Sheldon earthquake sequence in the far NW corner of Nevada. The sequence is characterized by bursts of activity growing in intensity leading to 47 events within one magnitude unit of the largest earthquake (Mw4.8). The closest station to the sequence when it began was NC network station MOD at about 50 km distance. NSL installed a portable telemetered broadband/SM instrument in November 2014 (NN_COLR), which is still in operation (remarkably with no follow-up site visits - 3 years of operation). This station is about 15 km epicentral distance from most of the sequence, placing it about within one focal depth of the activity. The third closest station, US network station WVOR,

is located in southern Oregon at Pn distances. Analysis of this sequence was also used in the testing and development of the GrowClust relocation method (Trugman and Shearer, 2017a).

3.4.1 Sheldon Earthquake Relocations

It is remarkable that we are able to achieve high-quality relocations sufficient to image the structures in great detail with such limited station coverage (see Figures 9 and 10). The vast majority of earthquakes in the sequence cannot be located, as they are only seen at two stations. Based on observations and the rates of M > 2 events, the Sheldon sequence has produced probably 50,000 M ~0 events. The completeness level is about M 1.8-2.0, after November 2014. This unusual sequence has produced 265 earthquakes M > 3.0, which includes 26 M > 3.95. MTINV moment tensor solutions were computed for ~70 events. Most show primarily down-to-the-east normal faulting with a component of oblique slip on a SSE steeply dipping (~70 degrees) structure. Despite the poor coverage, moment tensor orientations for the SSE dipping structure are consistent with the relocations. Considering the bursts of activity and the unusual number of M > 3 earthquakes, there was some concern that the sequence was driven by volcanic processes. There is no evidence from the seismicity or tendency for non-double couple sources to suggest volcanic processes are involved. Also, the seismicity and the moment tensor solutions suggest a well-defined fault surface, associated with a minor off-fault cluster at shallower depths. Earthquakes range in depth from about 10-13 km depth, typical of tectonic sources.

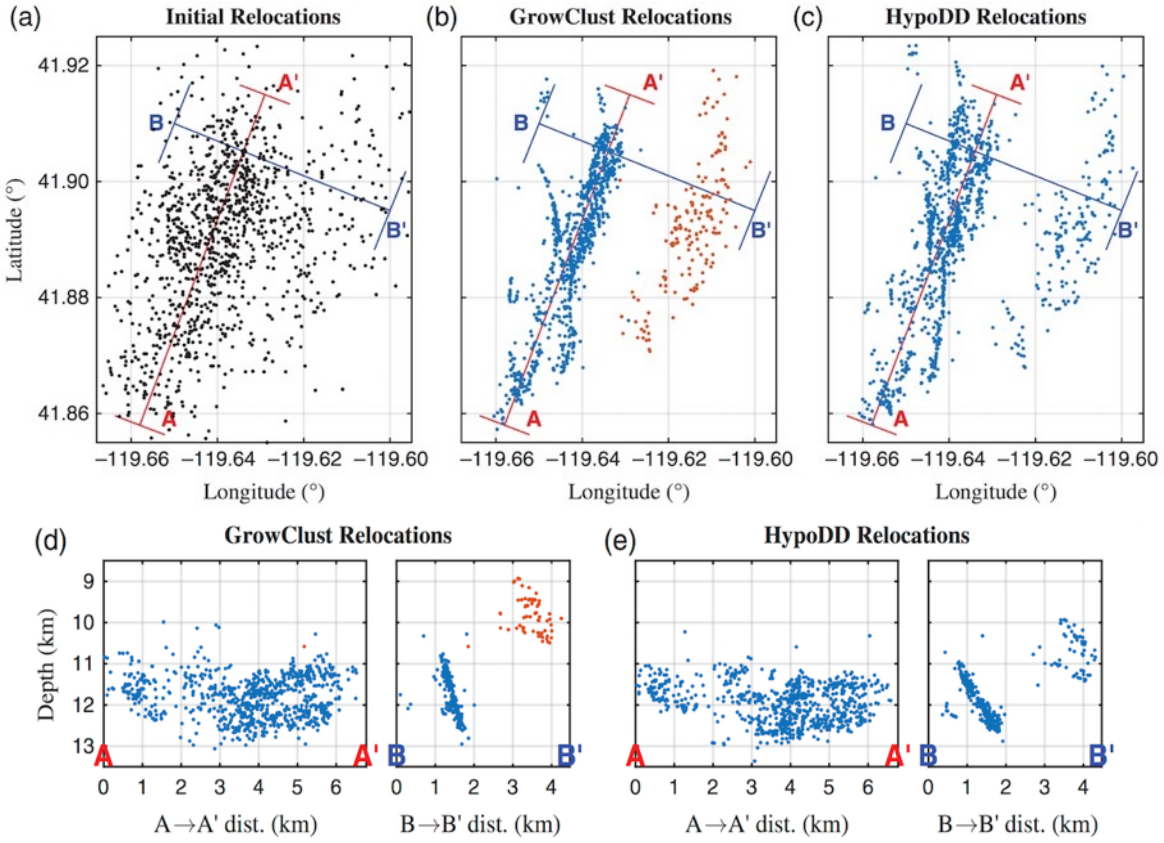

Figure 9. Relocation of the Sheldon sequence comparing catalog, GrowClust, and hypoDD locations, in map view (a-c) and cross-sections (d-e). Two clusters are imaged. Figure from Trugman and Shearer (2017a).

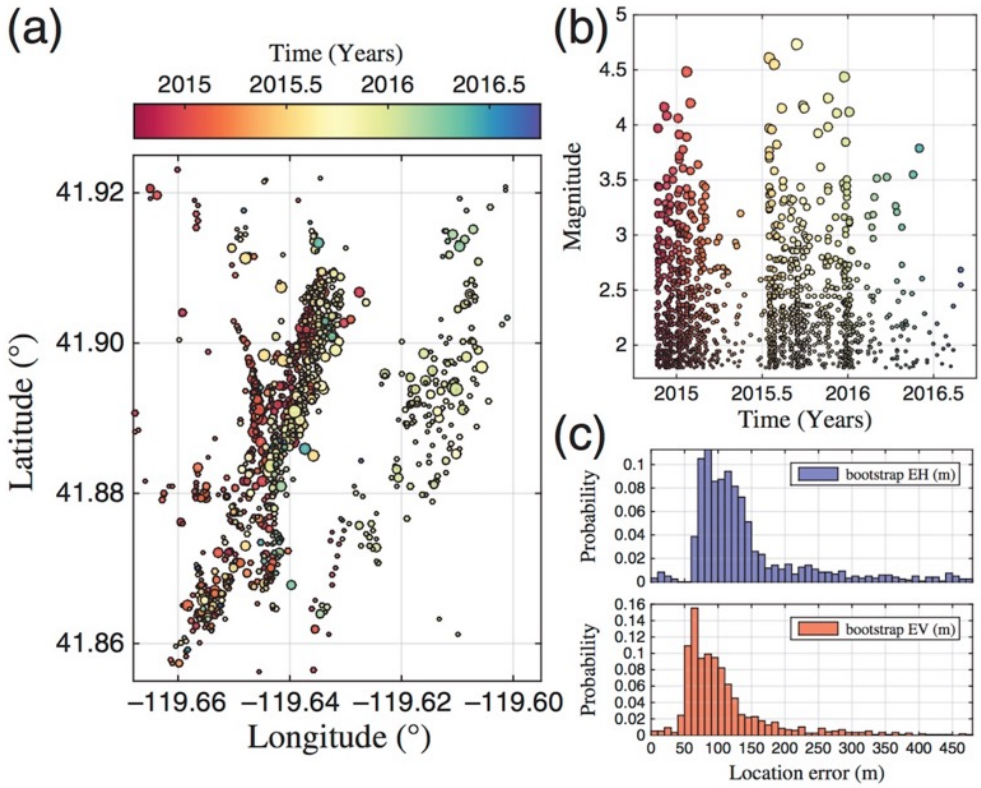

Figure 10. Temporal evolution of the Sheldon sequence showing the bursts of activity. Also shown are the location error estimates developed from GrowClust (figure from Trugman and Shearer, 2017a).

3.4.2 Moment Tensor Solutions

Of the 265 M > 3 events, 107 moment tensors were able to be calculated with MTINV. Figure 11 shows moment tensor solutions colored by estimated depth. These preliminary depths and locations have been updated with GrowClust. There is a clear tendency for a NNW-SSE trend.

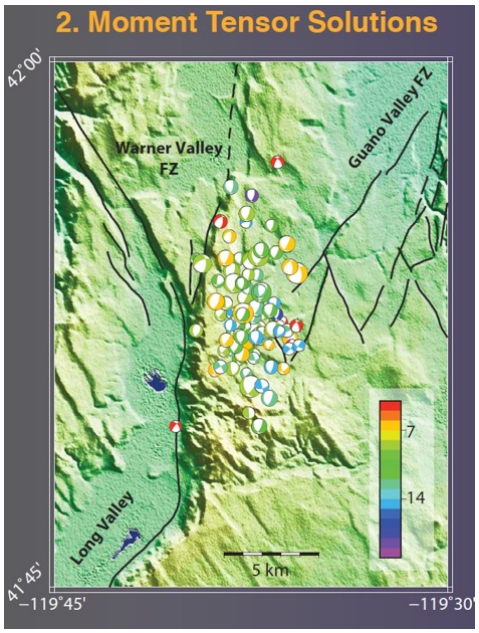

Figure 11. Moment tensor solutions for the 2014-2016 Sheldon sequence determined with MTINV.

3.4.3 Sheldon Stress Drop Analysis

We attempted to fit the corner frequency of 18 events greater than M_L 3.95 using a multiple empirical Green's function (EGF) method. We calculate spectra and spectral ratios for S-waves using the multi-taper method of Prieto et al. (2009), which allows easy visual examination of the source time function. We then perform a grid-search around the corner frequency of the large event to find the range of fc1 and fc2 in which the variance of the fit is within 5% of the minimum value. We do this for as many EGFs as fit our objective criteria then calculate an inverse-variance weighted mean to down-weight the measurements with large uncertainties.

For the Sheldon stress drop analysis; these objective criteria are considered:

- Large signal compared to pre-phase noise (SNR >= 3)
- High cross-correlation coefficient (f1 xcorr 0.70)
- Parabola shape with clear minimum (variance 0.005)
- Large amplitude range of model (difference in amp >= 3)
- Uncertainty in corner frequency fit (fc error <= 0.3)

Figure 12 illustrates the EGF fitting procedure for a Sheldon M 4.2 event and Figure 13 shows source parameter estimates versus seismic moment. Constrained results (blue) show no clear increase in stress drop with moment, although the results have considerable scatter around ~10 MPa (Figure 13, middle panel).

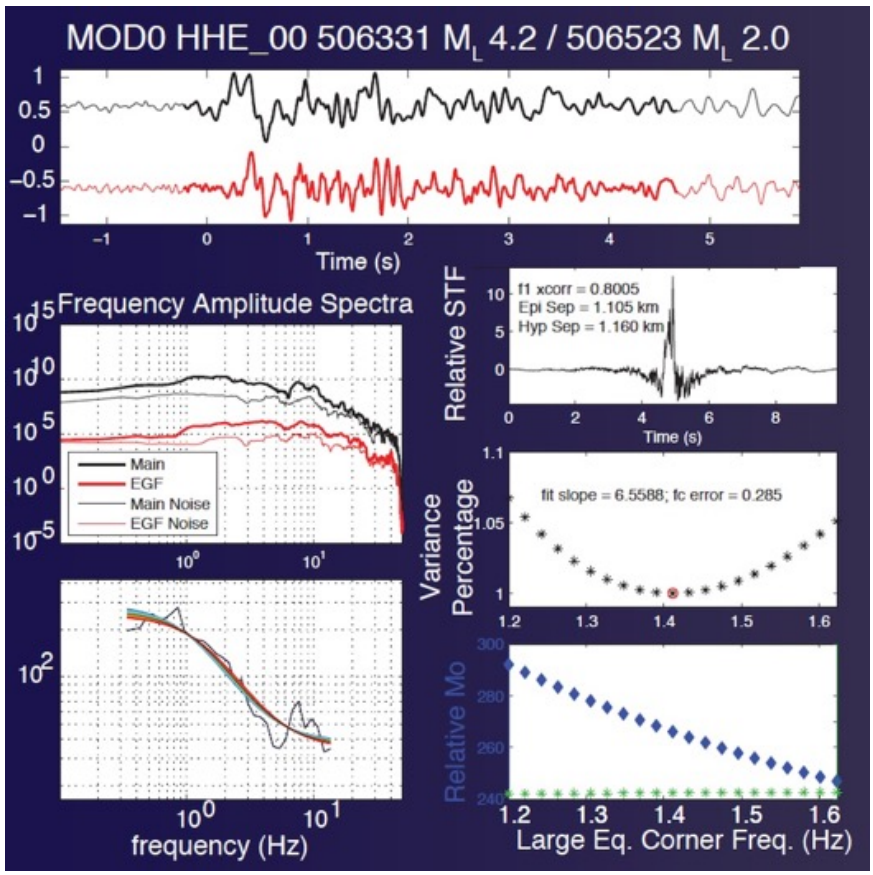

Figure 12. Example of a EGF selection for a Sheldon M 4.2 event based on cross-correlation criteria. Deconvolution STF, spectral ratio result and error estimates are shown.

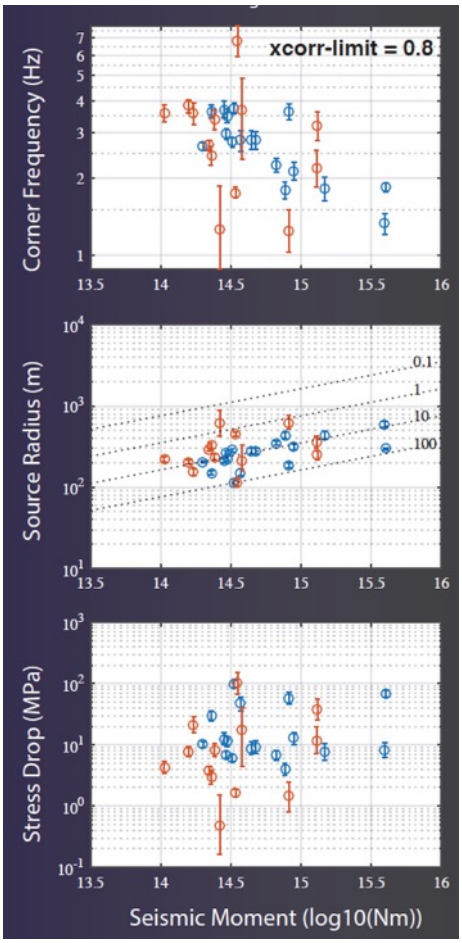

Figure 13. Corner frequency, source radius, and stress drop results for well-constrained earthquakes (blue) and poorly-fit earthquakes (red).

3.5 2016-2017 Nine Mine Ranch Sequence, 3 Mw ~5.5 Events West Central Nevada

On December 28th, 2016, three moderate sized earthquakes (Mw 5.6, 5.4, and 5.5) occurred within one hour in the central Walker Lane, near historic Nine Mile Ranch, ~30 southwest of Hawthorne, Nevada (Figure 14). The initial event, Mw 5.6 at 08:18 UTC, was followed 4 minutes later by an Mw 5.4 (08:22 UTC). The third, Mw 5.5 at 09:13 UTC, occurred 55 minutes after the initial moderate event. NSL moment tensor solutions for the three events are similar and show high-angle strike-slip faulting with an ENE-WSW extension direction. Summing the moment of the three main events equates to an M_w 5.9. These events resulted in surface cracks and damage to the recently refurbished house and out buildings of Nine Mile Ranch, historical late 1800s brick and stone structures (Figure 15). To date, the Nevada Seismological Laboratory (NSL) has located over 8500 events in this ongoing sequence. Including the three Mw ~ 5.5s, there have been 33 M >= 3 events and none in the M4 range. These are the largest earthquakes in the central Walker Lane Mina Deflection region since the 2003-2004 Adobe Hill earthquake sequence about 20 km to the SE, which also included 3 M ~5.5 events and an extended aftershock sequence.

3.5.1 Nine Mile Rance Earthquake Relocations

As in our analysis of other Nevada sequences, we develop a set of high-precision locations (for events located to date) with GrowClust, isolating the geometry of the complex structures within the sequence (see Figures 16 and 17). As with several other moderate size strike-slip faulting events in Walker Lane region the Nine Ranch sequence shows a conjugate strike-slip faulting geometry (see Ichinose et al. 1998 and references). Primary faulting in the Nine Mile Ranch sequence involved right lateral strike-slip motion on NW striking structure. Isolating the individual M ~5.5

moderate events to the conjugate structures within the sequence is problematic; each occurred near the intersection of obvious NW and SE striking structure determined from the relocations and all have similar mechanisms. This analysis is underway.

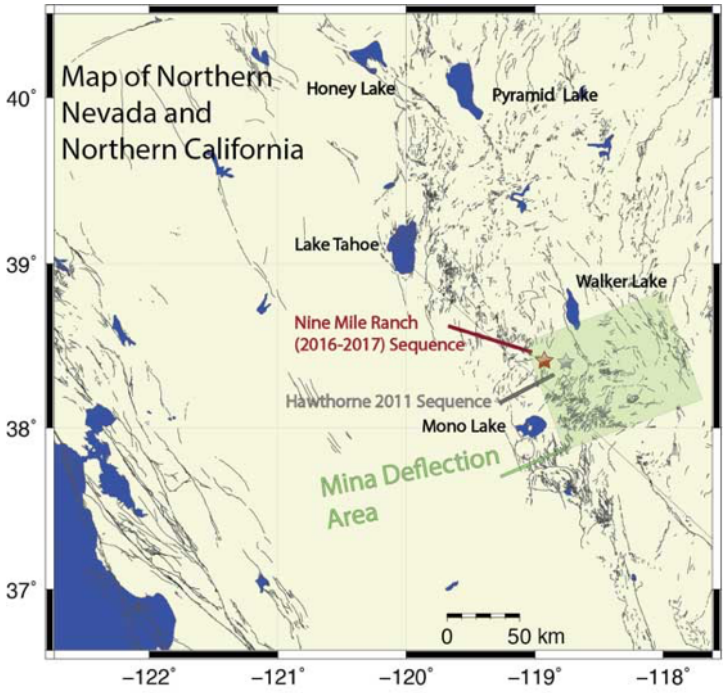

Figure 14. Location of the Nine Mile Ranch sequence in the central Walker Lane and Mina Deflection area. Mono Lake is located approximately 30 km to the south.

Figure 15. Damage to historical Nine Mile Ranch about 30 km SW of Hawthorne, Nevada. This historical building had recently been remodeled. It is reported that Mark Twain spent 10 days at Nine Mile Ranch in 1862 while living and mining in community of Aurora about 20 miles to the south. He stayed at Nine Mile Ranch with the son of then Governor of Nevada Nye.

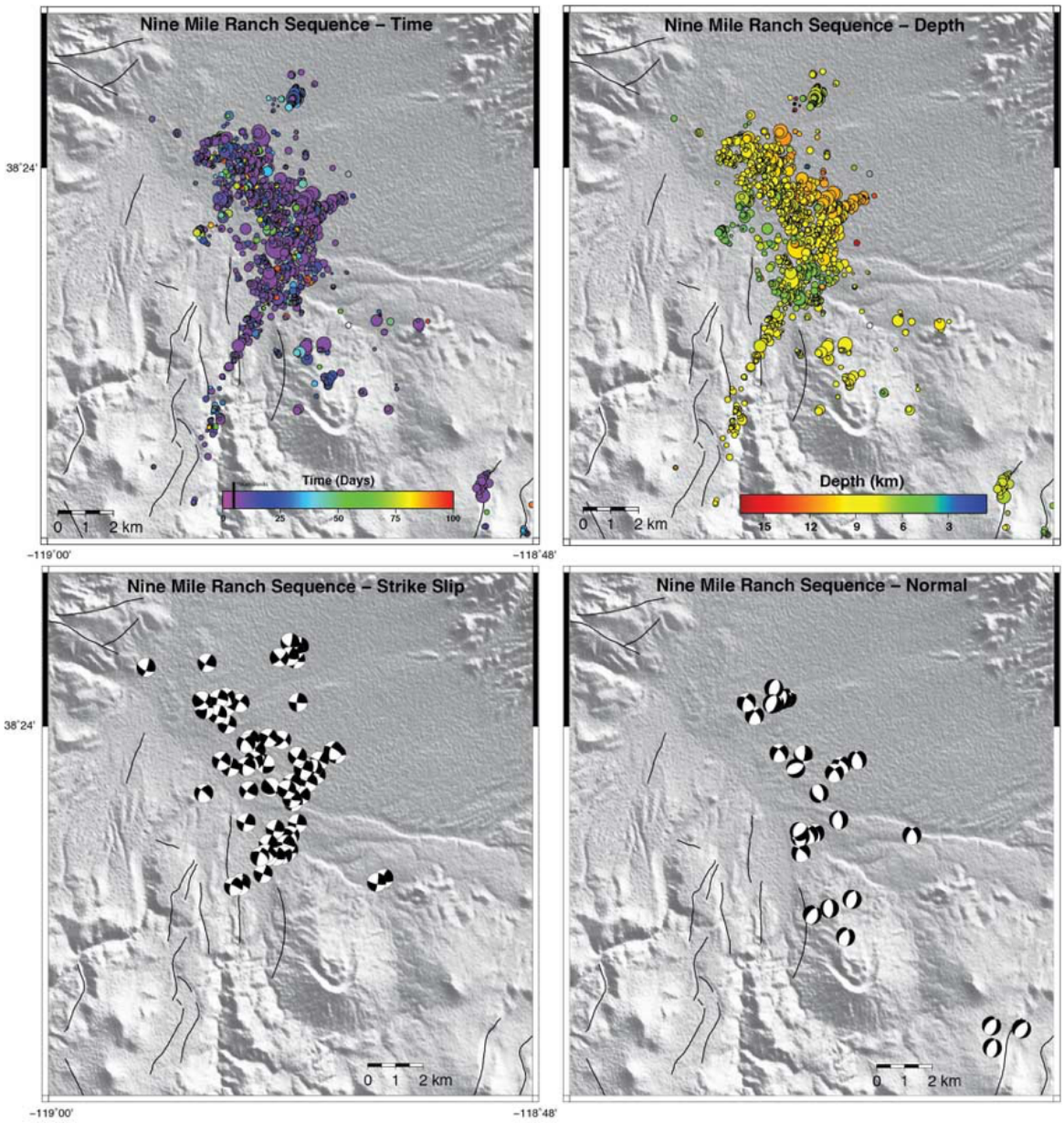

Figure 16. Map view of Nine Mile Ranch relocations, showing locations of the larger events and short-period focal mechanisms. A conjugate geometry is clear from map. The figure shows that the early period of the sequence was very energetic (upper left panel), and that earthquakes are occurring at typical seismogenic depths (upper right panel). HASH Focal mechanisms are separated in strike-slip (left lower panel) and normal (right lower panel) solutions.

3.5.2 Moment Tensor Solutions

Well-constrained moment tensor solutions for the 3 largest events are similar. Worth noting is the slight south-of-west (SSW orientation of the T-axis, this is unusual for most earthquakes in the west central Basin and Range (Ichinose et al., 2003) where the T-axis is oriented more EW or NW.

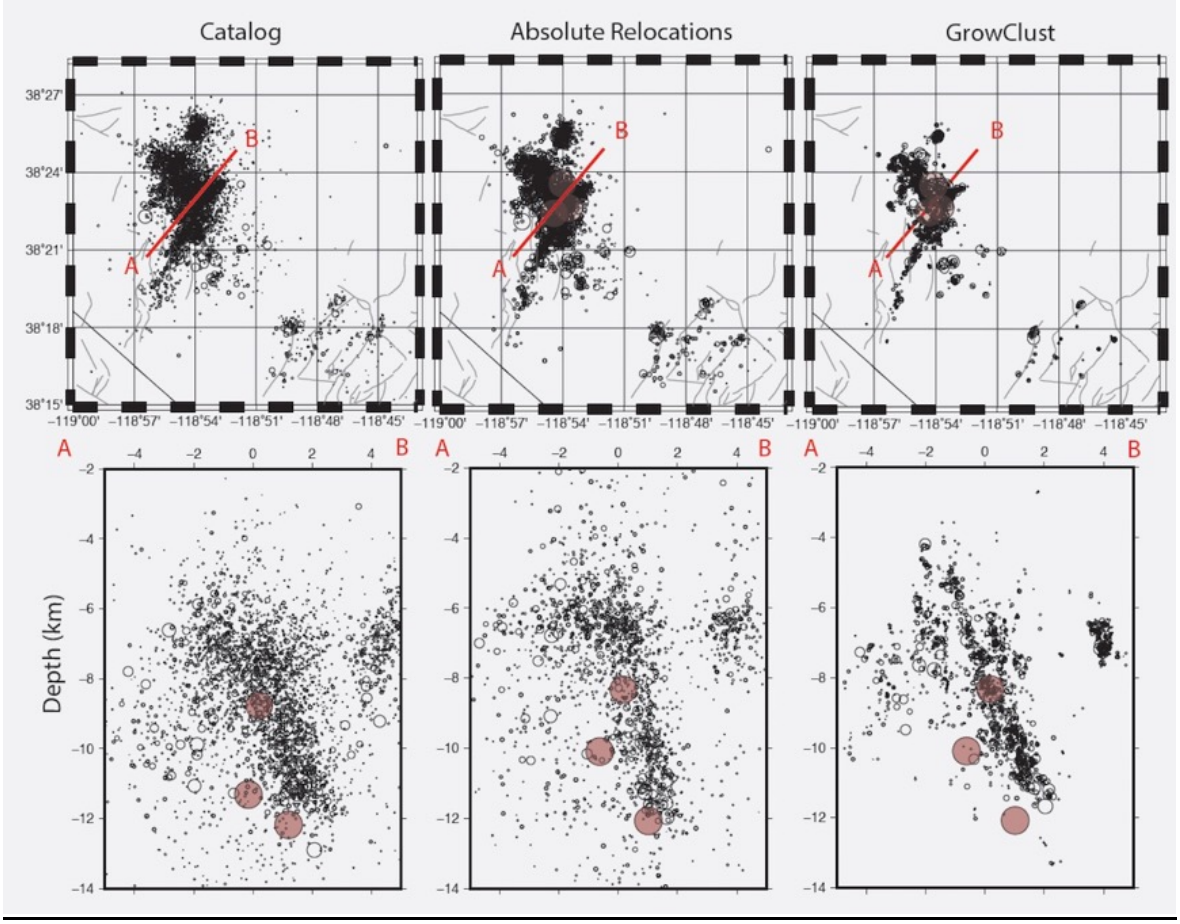

Figure 17. Comparison of catalog, HYPOINVERSE and GrowClust locations for the Nine Mile Ranch sequence. Lower panels are matching cross sections.

3.6 Stress Inversion in the Vicinity of the Nevada National Security Site

NSL has operated a seismic network in the vicinity of the Nevada National Security Site since late 1992 (see Figure 18). This was primarily in support of the Yucca Mountain Project and on-site monitoring has continued. Only events since 2000 are considered here, when only digital seismograph stations were used to develop the catalog. Not shown is the distribution of stations in early 2000s but the more recent configuration post-Yucca Mountain. Stations in the Death Valley area in eastern California are still operated as analog 70s era low dynamic range station.

During the Yucca Mountain monitoring period "all" earthquakes within a 65km radius of the Yucca site were located. Many of these included on only 5 or 6 stations in the location, therefore, many are poorly constrained. Also, most of the stations that were in place through approximately 2011, are currently not in operation. The heterogeneous nature of the network limits the cross-correlation technique for more recent events.

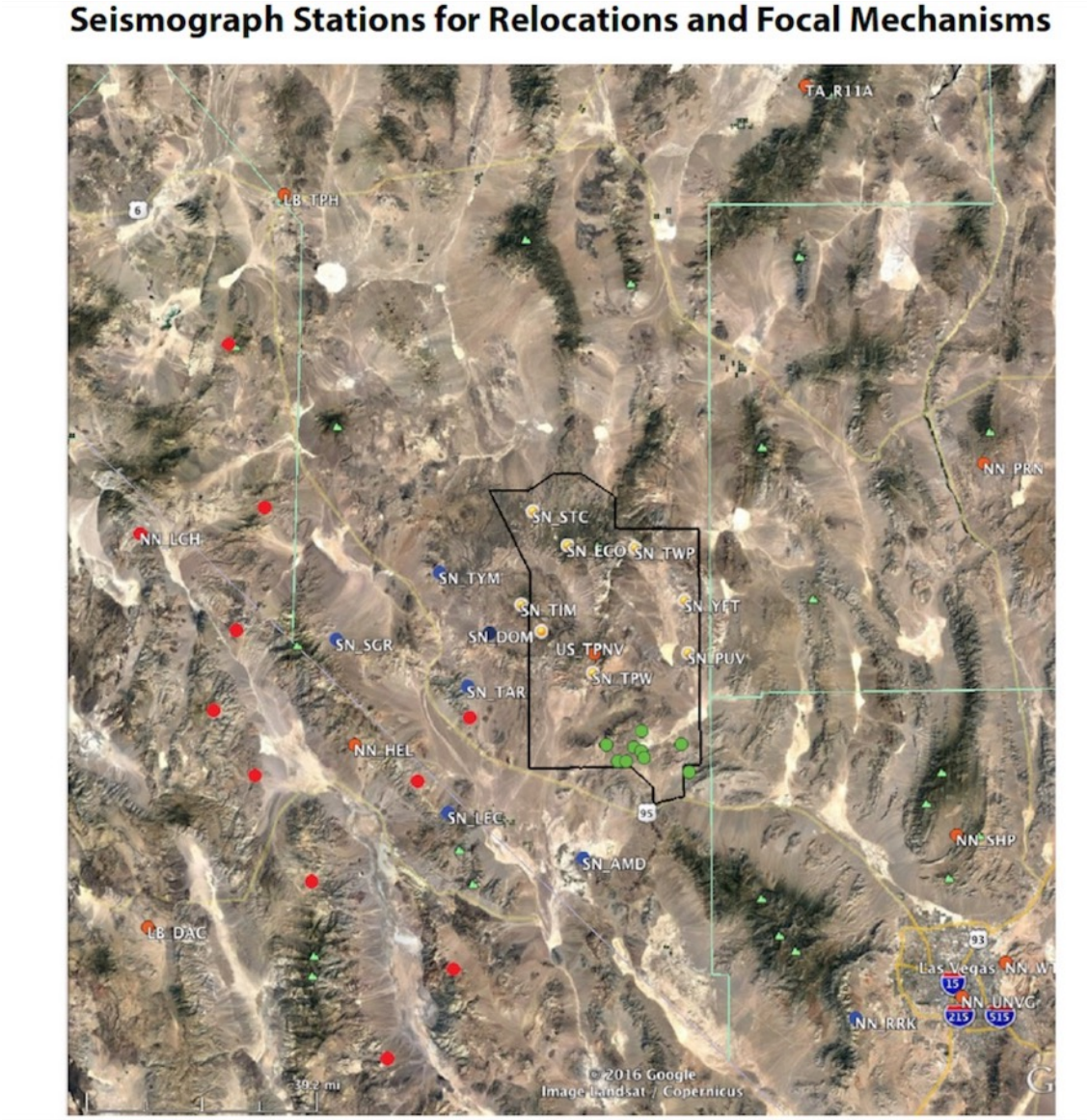

Figure 18. Most recent distribution of seismograph stations in the NNSS area (formerly NTS). The network, since 1992, has experience many changes and upgrades. Therefore, there is a heterogeneous set of event-station pairs to develop high-precision locations. In addition, coverage is very uneven throughout the southern Nevada area. Stations operated outside of NNSS have been recently supported under USGS network operations agreements.

A comprehensive set of relocations in under development; network coverage is heterogeneous in both time and space. However, for the southern Nevada southeastern California region SATSI stress inversion, a total of 2048 short period focal mechanisms were compiled (Figure 19). Of these 707 were acquired from prior NSL NNSS area reports (1992-2000). Most of these focal mechanisms were computed with program FPFIT (Reasenburg and Oppenheimer, 1985). These also include early mechanisms (1978-191) derived from USGS reports, prior to NSL's operation of the Southern Great Basin network. Also, some HASH derived mechanisms on NNSS were computed in the Reeves et al. (2016) study. The remainder were computed using HASH from analyst first motions picks from 2000 to present for this study and cover a wider region. These

mechanisms sample a broad region of southern Nevada and southeast California. The most sampled area is the SW NNSS area; these are primarily aftershocks of the 1992 Little Skull Mountain earthquake. Due to the general sparse station coverage in the region (except for some areas of NNSS) most focal mechanisms are poorly constrained. Mechanisms with a positive rake angle greater than 20 degrees for both fault planes in the solutions were excluded. Reverse mechanisms are interpreted to result from incorrect analyst first motion picks or poorly constrained solutions in this transtensional tectonic environment. Reverse mechanisms are not observed in analyst reviewed mechanisms. Most of these mechanisms, particularly those developed since 2011 have not been formally reviewed; first motions are taken directly from the NSL database.

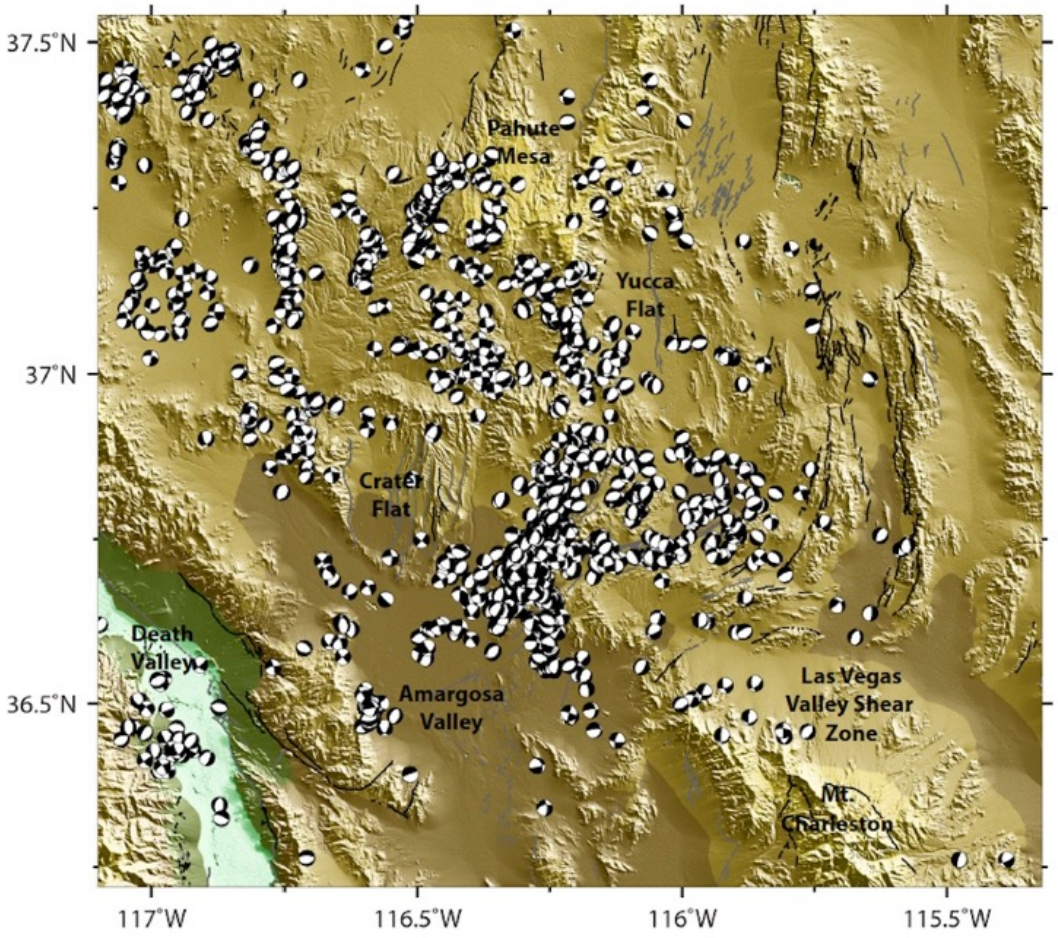

Figure 19. Focal mechanisms compiled from southern Nevada monitoring. Several routines were used to determine and compile the focal mechanisms over the monitoring history.

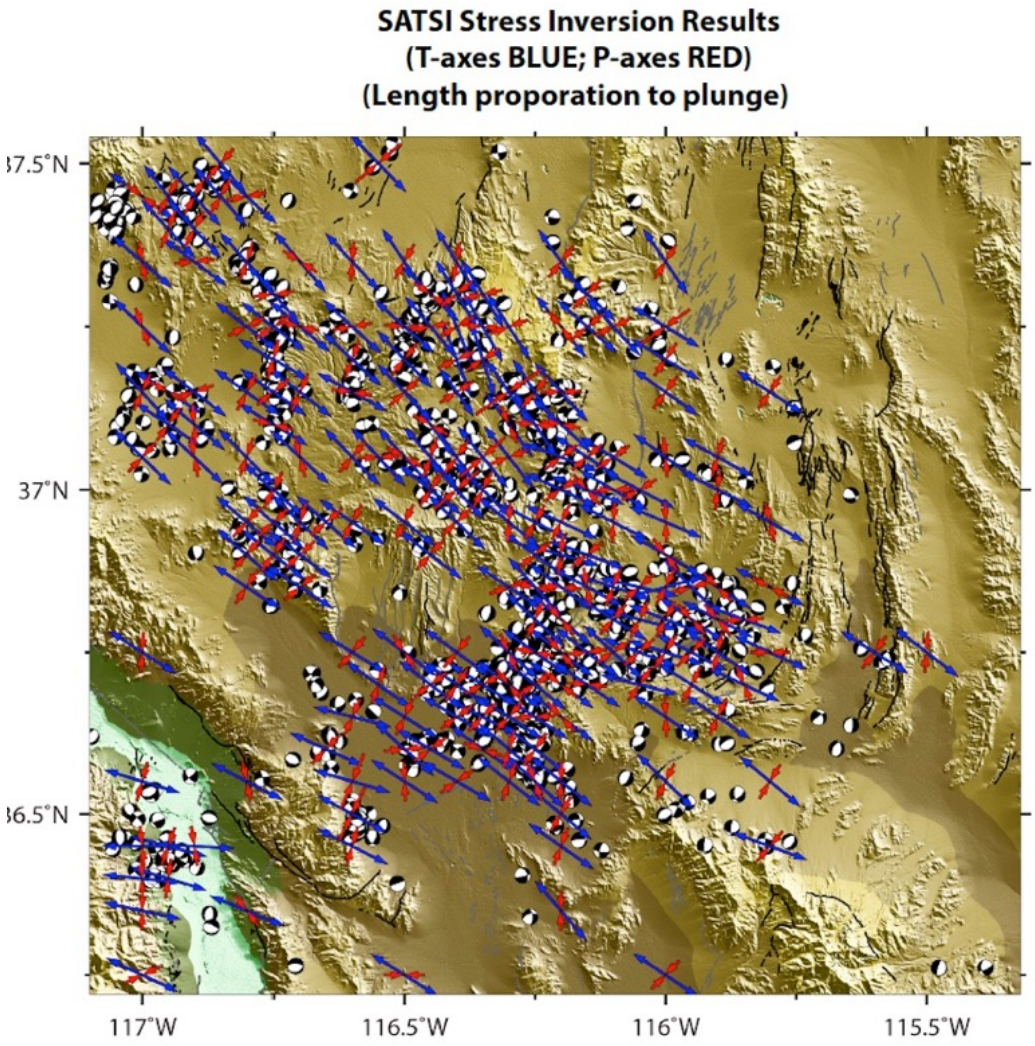

Figure 22. SATSI stress inversion results. With T-axes "blue" and P-axes "red". Length of the axis is proportional to plunge.

SATSI's damped inversion technique forces a solution constrained to adjacent grid points, assuring a result that is both smooth as well as accommodating local variability in the stress field. Although SATSI can be used for temporal and 3D stress variations, only the 2D case is used here. Because of the sparse sampling of the available focal mechanisms in the northwest NNSS area, a pseudo smoothing strategy was applied to capture both the regional stress field as well as the local stress variations from local clusters of resolvable mechanisms. SATI was run with various grid spacing in order to capture the details of the stress field that are sampled without incorporating data from areas that were poorly sampled. A grid spacing of 0.5 degrees, 0.1 degrees, 0.050 degrees, and 0.025 degrees were applied in individual stress inversions. A solution with the smallest grid spacing, satisfying at least three mechanisms per grid, was taken as the best solution for that location and took precedent over coarser SATSI grid spacing results. In this way, all mechanisms contribute to the final stress field estimate.

The resulting solution shows a distinct rotation in the regional T-axis in central NNSS, near the Timber Mountain Caldera complex where the T-axis rotates clockwise from WNW in southeast Nevada to approximately NW approaching the southern Walker Lane regional fault systems.

3.7 Relocations, Moment Tensors and Focal Mechanisms-Western Great Basin

Preliminary GrowClust relocations have been computed for northwest Nevada and along the eastern Sierra between Lake Tahoe and Mammoth Lakes (Figure 23) for earthquakes since 2000. It is apparent that the optimum strategy is to isolate regions for relocation and cluster identification rather than relocate large regions in one step; however, this step allows us to isolate areas and clusters for further analysis. Missing below is much of west central Basin and Range and the Mina Deflection, which require more attention. This exercise illustrates the Nevada regional large data set, even since 2000, and numbers of individual clusters and regions of well-defined seismicity yet to be studied.

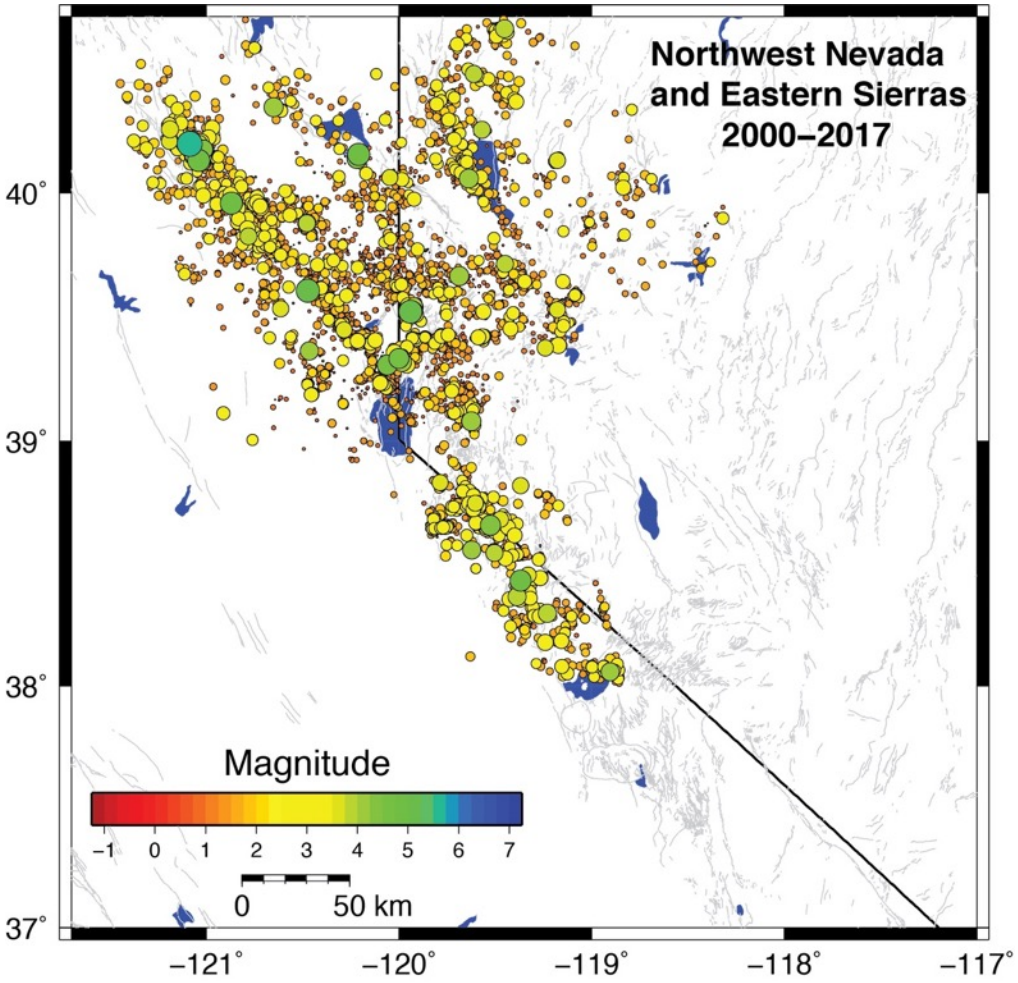

Figure 23. 23,000+ relocated events within NW Nevada and eastern Sierras, from 2000-2017. Events are colored and sized by magnitude. Grey lines are faults from the USGS Faults and Folds database.

In preparation for the regional stress inversion ~4000 short-period mechanisms have been computed with HASH in the western Basin and Range. The NSL database of 320 moment tensor solutions since 2011 are also included in Figure 24, below. This is ongoing work.

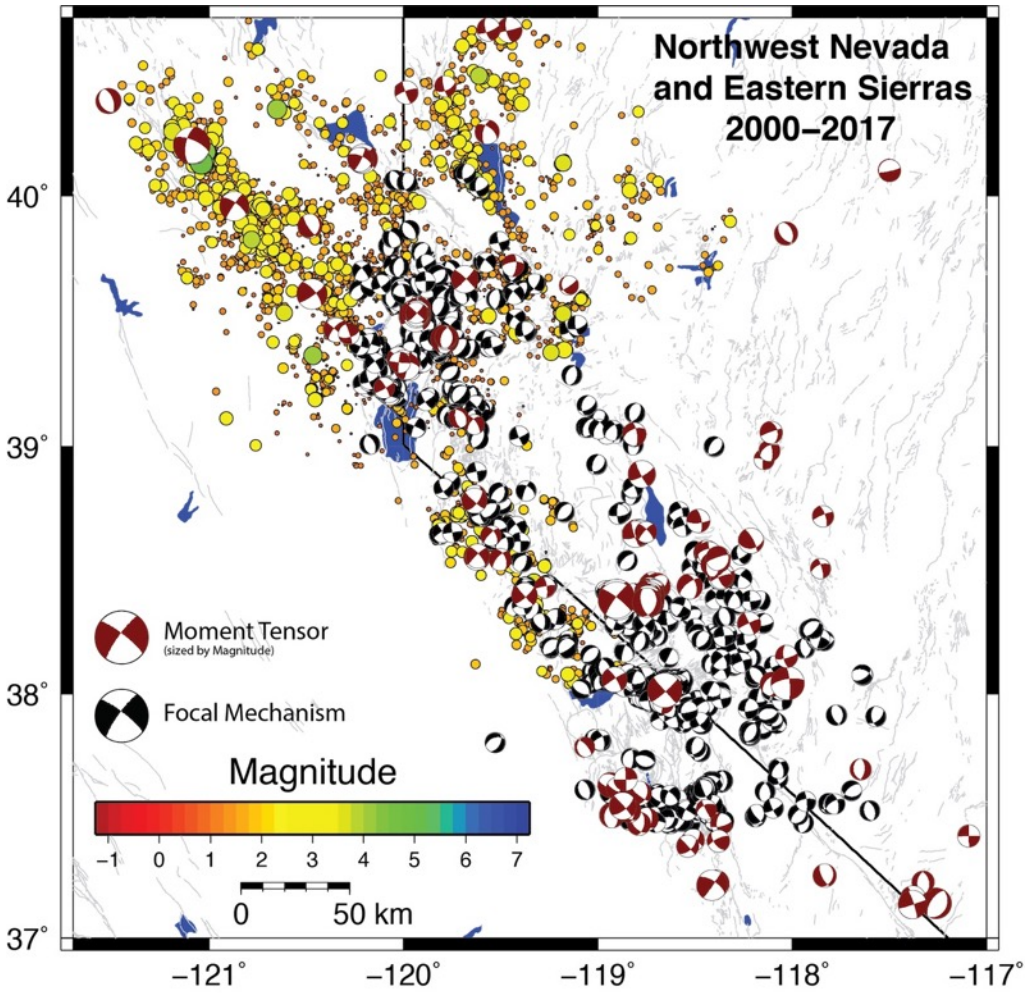

Figure 24. ~4000 short-period first motion HASH focal mechanisms and 320 moment tensor solutions shown with NW Nevada and eastern Sierra relocations.

3.8 Continuing Studies Highlighted During the Course of Study:

The recent **Virginia City** earthquake sequence, primarily throughout 2014 included three M 3 event but also a complex set of triggered faults within the small sequence (Hatch et al., 2016). A detailed analysis is ongoing using GrowClust locations and short-period mechanisms to isolate the active structures and the evolution of the sequence not completed. Following the damaging 2008 Mogul, west urban Reno sequence, local emergency community conducted daily conference calls in planning scenarios in the event of a large earthquake associated with the sequence. This series of M 3s is also significant as the structural details in Virginia City, Nevada area is difficult to access, and damage to local roads would create a challenge to response.

The December 2015 Mw 4.3 **Thomas Creek** earthquake sequence in southeast Reno was widely felt throughout the urban area (Hatch et al. 2016). The normal faulting Mw 4.3 mainshock was preceded for 20 minutes by a high rate of activity that included 3 M 3 events; the mainshock and all M3s in the foreshock period were strongly felt in south Reno area. Hatch et al. (2016) determined the sequence occurred on the west dipping Virginia Range frontal fault along the east side of the

Reno basin; this is significant due to the controversy regarding of the presence of an active west dipping basin bounding structure in the south Reno area.

The Mw 4.3 2016 **Herlong,** California earthquake and sequence occurred on the Honey Lake fault zone (Hatch et al., 2016). The Honey Lake fault zone is one of the primary northern Walker Lane right-lateral strike slip systems and is capable of earthquakes of near M 7.

4.0 Conclusions:

A significant amount of work has been accomplished in this initial Phase of a much larger effort to analyze Nevada region seismicity and earthquake clusters/sequences. We have been able to streamline several methods of analysis that have been adapted to the NSL Antelope database, many of these techniques been directly developed or improved under this study. The Nevada region has a wealth of seismicity for taking this integrated approach in applying modern methods for comprehensive seismotectonic and source parameter analysis in a transtensional tectonic environment. The details of many Nevada sequences require comprehensive detailed studies that can address the complexities and variety of faulting and clustering processes that are characteristic of most Nevada earthquake sequences. Considering the scope of the research, this initial effort has focused on more effectively adapting techniques and applications (e.g., GrowClust, HASH, SATSI, EGF methods, STF directivity, etc.) for efficient analysis of small but very energetic sequences. Improvement in the Nevada and eastern California network under USGS support in recent years has proven invaluable in evaluating recent regional sequences. Phase II of the program will continue the analysis of the characteristics of Nevada seismicity, completing ongoing study of energetic sequences in the Reno-Carson City-Truckee-Lake Tahoe area, assessing the seismicity along the eastern Sierra south of Reno-Lake Tahoe, and areas of persistent seismicity in the southern Nevada region.

Reviewed Publications Related to this Study:

Ruhl, C. J., R. E. Abercrombie, and K. D. Smith (2017), Spatiotemporal variation of stress drop during the 2008 Mogul, Nevada earthquake swarm, *J. Geophys. Res.*, doi:10.1002/2017JB014601.

Ruhl, C. J., R. E. Abercrombie, K. D. Smith, and I. Zaliapin (2016), Complex spatiotemporal evolution of the 2008 Mw 4.9 Mogul earthquake swarm (Reno, Nevada): interplay of fluid and faulting, *J. Geophys. Res. Solid Earth, 121,* doi:10.1002/2016JB013399.

Ruhl, C. J., T. C. Seaman, K. D. Smith, and G. M. Kent (2016), Seismotectonic and seismic hazard implications for the Reno-Tahoe area of the Walker Lane in Nevada and California from relocated seismicity, first-motion focal mechanisms, moment tensors, and variations in the stress field, in Applied Geology in California, AEG Special Volume, eds. R. Anderson and H. Ferriz.

Trugman, D. T. and Shearer, P.M. (2017a). GrowClust: A Hierarchical Clustering Algorithm for Relative Earthquake Relocation, with Application to the Spanish Springs and Sheldon, Nevada, Earthquake Sequences, Seism. Res. Lett., 88, September 2017.

Aberombie, R.E., Poli, R., Bannister, S. (in press). Earthquake directivity, orientation and stress drop within the subduction plate at the Hikurangi margin, New Zealand, J. Geophs. Res., doi: 10.1002/2017JN014935.

Manuscripts in Preparation:

Hatch, R.L., Smith, K.D., Abercrombie, R.E., Ruhl, C.J., (2018). Mw 3.65 and Mw 3.85 earthquakes and aftershock sequence near Truckee, California, 2017: relocations, source parameters and directivity.

Hatch, R.L., Abercrombie, R.E., Smith, K.D., Ruhl, C.J., (2018). The 2010-2016 Virginia City, Nevada earthquake sequence; evolution of a complex faulting sequence and emergency response process.

Hatch, R.L., Abercrombie, R.E., Smith, K.D., Ruhl, C.J., (2018). Recent earthquake sequences along the eastern Sierra; the 2015 urban Reno, Nevada Thomas Creek sequence, main event Mw 4.5, the 2016 Honey Lake sequence, main event Mw 4.6, and the 2012 Carson City sequence, main event Mw 2.9; event relocation, source parameters and western Basin and Range seismotectonics.

Hatch, R.L., Abercrombie, R.E., Smith, K.D., Ruhl, C.J., (2018). The 2016-2017 Nine Mile Ranch sequence central Nevada; 3 Mw ~5.5 events and complex faulting earthquake sequence.

Ruhl, C.J., Abercrombie, R.E., Smith, K.D. (2018). Characterizing three years of seismic unrest at the Sheldon Antelope Refuge in far northwest Nevada.

Abercrombie, R. E. and C. J. Ruhl (*in prep.*), Directivity of M2.2-5 Earthquakes in the Shallow Mogul Earthquake Swarm, Reno, Nevada.

Ruhl, C. J., K. D. Smith, G. M. Kent, and R. E. Abercrombie (*in prep.*), Seismicity Patterns in the Vicinity of Reno, Nevada Reflect Changes in Crustal and Faulting Properties between the Sierra Nevada Block and the Basin-and-Range Province.

Posters/Abstracts Professional Meetings:

Hatch, R.L., Ruhl, C.J., Trugman, D.T., Smith, K.D. (2016). Event relocations, focal mechanisms, and source parameters of recent earthquakes in the Reno, Nevada urban areas, EOS Am. Geophysical Annual Meeting 2016, Abstract #: S13A-2519, San Francisco.

Hatch, R. L., Ruhl. C.J., Brailo, C., Smith, K.D., Louie, J.L., Kent, G.M., Rodgers, A. (2016). The MW 4.3 December 22, 2015 Thomas Creek earthquake, south Reno, Nevada, *Seism. Res. Lett,* Seismological Society of Am. Annual Meeting, Reno, Nevada.

Hatch, R. L., Ruhl, C. Trugman, D., Smith, K., Shearer, P., Abercrombie, R. (2016), Characterizing Seismicity with High-Precision Relocations of Recent Earthquake Sequences in Eastern California and Western Nevada, *SCEC Annual Meeting, Sept. 2016, (Poster) Palm Springs, CA*

Hatch, R. L., Ruhl, C. Trugman, D., Smith, K., Shearer, P., Abercrombie, R. (2016), Event Relocations, Focal Mechanisms and Source Parameters of Recent Earthquake Sequences in the Reno, Nevada Urban Areas, *American Geophysical Union, Fall Meeting, Dec. 2016, (Poster) San Francisco, CA*

Hatch, R. L., Ruhl, C. Trugman, D., Smith, K., Shearer, P., Abercrombie, R. (2017), Characterizing Recent Northern Walker Lane Earthquake Sequences: Complexities in Geometry and Sources Processes, *Seismology Society of America Annual Meeting, 2017, (Poster) Denver, CO*

Hatch, R. L., Ruhl, C., Smith, K., Abercrombie, R. (2017), Moderate Sized Events (3 Mw 5.4-5.6) and Aftershock Relocations of the 2016-2017 Nine Mile Ranch Earthquake Sequence near Hawthorne, Nevada *Seismology Society of America Annual Meeting, April 2017, (Poster) Denver, CO*

Hatch, R. L., Smith, K., Abercrombie, R. (2017), Analysis of Two Magnitude ~4 Earthquakes and Aftershocks Near Truckee, California, 2017 *SCEC Annual Meeting, Sept. 2017, (Poster) Palm Springs, CA*

Hatch, R. L., Smith, K., Abercrombie, R. (2017), Analysis of Two Magnitude 3.5+ Earthquakes and Aftershocks Near Truckee, California, 2017 *Graduate Student Association Poster Symposium, Fall 2017, Reno, NV*

Rodgers, A.J., Louie, J.L., Smith, K.D., Ruhl, C.J., Brailo, C. Kent, G.M., Pullammanappllil, S. (2016). Ground motion simulations of the December 22, 2015 Thomas Creek earthquake, south Reno, including 3D basin structure, *Seism. Res. Lett,* Seismological Society of Am. Annual Meeting, Reno, Nevada.

Ruhl, C. J., R. E. Abercrombie, K. D. Smith (2017), High-resolution spatial variation of stress drops illuminates shallow fault zone behavior in the 2008 Mogul earthquake swarm (Nevada), Abstract presented at the 2017 Earthscope National Meeting, Anchorage, AK, 16-18 May.

Ruhl, C. J., K. D. Smith, and R. E. Abercrombie (2016), Moderate-to-small magnitude seismicity clusters persist in Northwest Nevada for over 19 months, Abstract presented at the 2016 SSA Annual Meeting, Reno, NV, 20-22, Apr,

Ruhl, C.J., Abercrombie, R.E, Smith, K.D. (2016) Variability of source parameter estimates for the 2008 Mogul earthquake swarm near Reno, NV using EGF derived spectral ratios, *Seism. Res. Lett,* Seismological Society of Am. Annual Meeting, Reno, Nevada.

Smith, K.D., Hatch, R.L., Trugman, D.T., Shearer, P.M. (2016). High-resolution relocations of digital-era seismicity and stress estimates in the vicinity of the Nevada National Security Site, southern, Nevada, EOS Am. Geophysical Annual Meeting 2016, Abstract #: S13A-2816, San Francisco.

Smith, K.D., Ruhl, C.J., Kent, G.M. (2016). Review of the seismotectonics, historical and instrumental seismicity of Nevada and eastern California, S*eism. Res. Lett,* Seismological Society of Am. Annual Meeting, Reno, Nevada.

Trugman, D.T., Shearer, P.M., Smith, K.D. (2016) GlowClust: A hierarchical cluster algorithm for relative earthquake relocation, with application to the Spanish Springs and Sheldon, Nevada earthquake sequences, EOS Am. Geophysical Union Annual Meeting 2016, Abstract #: S13A-2815, San Francisco.

Invited Presentations - Christine Ruhl (resulting from studies conducted directly or utilizing results from this research grant):

Ruhl, C. J., R. E. Abercrombie, R. L. Hatch, and K. D. Smith (2017), Seismicity, Stress Drop, and Directivity Patterns observed in Small-Magnitude (<M5) Earthquake Sequences near Reno, Nevada, Invited talk presented to the Seismology Seminar at Department of Geosciences, University of Oregon, Eugene, Oreg., 1 Dec.

Ruhl, C. J., R. E. Abercrombie, K. D. Smith, I. Zaliapin (2017), Complex Spatiotemporal Evolution of Seismicity and Source Parameters of the 2008 Mw 4.9 Mogul Earthquake Swarm in Reno, Nevada, *Invited* talk presented to the Solid Earth Physics Seminar series at Harvard University, Cambridge, Mass., 15 Feb.

Ruhl, C. J., R. E. Abercrombie, K. D. Smith, I. Zaliapin (2017), Complex Spatiotemporal Evolution of Seismicity and Source Parameters of the 2008 Mw 4.9 Mogul Earthquake Swarm in Reno, Nevada, *Invited* talk presented at Earthquakes Science Seminar at the United States Geological Survey, Menlo Park, Calif., 1 Feb.

Ruhl, C. J., R. E. Abercrombie, K. D. Smith, I. Zaliapin (2017), Complex Spatiotemporal Evolution of Seismicity and Source Parameters of the 2008 Mw 4.9 Mogul Earthquake Swarm in Reno, Nevada, Invited talk presented at the New Mexico Institute of Mining and Technology, Socorro, New Mexico 17 Jan.

Ruhl, C. J., R. E. Abercrombie, K. D. Smith, I. Zaliapin (2016), Inside an Earthquake Swarm: Detailed Analysis of the 2008 Mogul Earthquakes in Reno, NV, Invited talk presented at Berkeley Seismological Laboratory Seminar, University of California, Berkeley, Berkeley, Calif., 25 Oct.

Associated Studies/Publications Utilizing Results from this Study or Data Derived from USGS Seismic Network Data and Supported Activities:

Brailo, C.M., Kent, G.M., Wesnousky, S.G., Hammond, W.C., Kell, A.M., Pierce, I.K., Ruhl. C.J., Smith, K.D. (2016). A LIDAR and GPS study of the greater Truckee Meadows: evidence for a

district transition from primarily east-west dominated extension to NW-trending right-lateral slip centered in Reno, Nevada, *Seism. Res. Lett,* Seismological Society of Am. Annual Meeting, Reno, Nevada.

Louie, J., Schmauder, G., Kent, G., Smith, K.D.,McBean, K., McBean A., Hall, K. (2016). Simulation of Scenario – Earthquake Shaking in the Lake Tahoe Basin – a Comparison Between ShakeMap and Nevada ShakeZoning, *Applied Geology in California* is the Association of Environmental & Engineering Geologists (AEG) Special Publication Number 26, Chapter 45, editors, Bob Anderson and Horacio Ferriz, Star Publishing Company, Inc., California.

Kent, G.M., Smith, K.D., Slater, D., Plank, G., Williams, M., Vernon, F. Driscoll, N.W. (2016). A-21st Century approach to firefighting in the western US: how microwave-based seismic networks can change fire suppression from reactive to proactive, *Seism. Res. Lett,* Seismological Society of Am. Annual Meeting, Reno, Nevada.

Kent. G., Schmauder, G., Maloney, J., Driscoll, N., Kell, A., Smith, K.D., Baskin, R., Seitz, G. (2016). Reevaluating Late-Pleistocene and Holocene Active Faults in the Tahoe Basin, California-Nevada, *Applied Geology in California* is the Association of Environmental & Engineering Geologists (AEG) Special Publication Number 26, Chapter 42, editors, Bob Anderson and Horacio Ferriz, Star Publishing Company, Inc., California.

Reeves, D.M., Smith, K.D., Parashar, R., Heintz, M.K. (2016). Determining the potential role on preferential flow and transport at Pahute Mesa, Nevada National Security Site, EOS Am. Geophysical Annual Meeting 2016, Abstract #: H51C-1481, San Francisco.

Reeves, D.M., Smith, K.D., Rarahar, R., Collins, C., HeintZ, K.M. (2016). Investigating the Influence of Regional Stress of Fault and Fracture Permability at Pahute Mesa, Nevada National Security Site, special study prepared for the Nevada Site Office, National Nuclear Security Administration, U.S. Department of Energy Las Vegas, Nevada, pp. 107.

Smith, K. D., G. M. Kent, D. P. von Seggern, N. W. Driscoll, and A. Eisses (2016), Evidence for Moho-lower crustal transition depth diking and rifting of the Sierra Nevada microplate, Geophys. Res. Lett., 43, doi:10.1002/2016GL070283.

Smith, K.D., Kent, G, Slater, D., Plank, G., Williams, M., McCarthy, M.I., Vernon, F., Werner-Braun, H., Driscoll, N. (2016). Integrated Multi-Hazard Regional Networks: Earthquake Warning/Response, Wildfire Detection/Response, and Extreme Weather Tracking, *Applied Geology in California* is the Association of Environmental & Engineering Geologists (AEG) Special Publication Number 26, Chapter 33, editors, Bob Anderson and Horacio Ferriz, Star Publishing Company, Inc., California.

Technical Report References:

Abercrombie, R. E. (2015), Investigating uncertainties in empirical Green's function analysis earthquake source parameters, *J. Geophys. Res.,* doi:10.1002/2015JB011984.

Abercrombie, R. E. (2014), Stress drops of repeating earthquakes on the San Andreas fault at Parkfield, *Geophys. Res. Lett., 41*, 8784-8791, doi: 10.1002/2014GL062079.

Abercrombie, R. E. (2013), Comparison of direct and code wave stress drop measurements for the Wells, Nevada, earthquake sequence, *J. Geophys. Res., 118,* 1458-1470, doi: 10.1029/2012JB009638.

Abercrombie, R. E., S. C. Bannister, J. Ristau, and D. Doser (2017), Variability of earthquake stress drop in a subduction setting, the Hikurangi Margin, New Zealand, *Geophys. J. Int., 208* (1), 306-320.

Argus, D.F. and Gordon, R.G. (1991). Current Sierra Nevada-North America motion from very long baseline interferometry: Implications for the kinematics of the western United States, Geology, 19, 1085-1088.

Busby, C.J. (2013). Birth of a plate boundary ca. 12 Ma in the ancestral Cascades arc, Walker

Lane belt of California and Nevada, Geosphere v. 9, 1147-1160,

Eshelby, J. D. (1957), The determination of the elastic field of an ellipsoidal inclusion and related problems, *Proc. Roy. Soc. Lond., A, 241,* 376-396.

Faulds, J.E., and Henry, C.D. (2008). Tectonic influences on the spatial and temporal evolution of the Walker Lane: An incipient transform fault along the evolving Pacific – North American plate boundary, *in* Spencer, J.E., and Titley, S.R., eds., Ores and orogenesis: Circum-Pacific tectonics, geologic evolution, and ore deposits: Arizona Geological Society Digest 22, p. 437-470

Faulds, J.E., Henry, C.D., and Hinz, N.H. (2005). Kinematics of the northern Walker Lane: An incipient transform fault along the Pacific – North American plate boundary: Geology, v. 33, no. 6, p. 505-508.

Hauksson, E. and P. Shearer, (2005) Southern California hypocenter relocation with waveform cross-correlation, Part 1: Results using the double-difference method, *Bull. Seismol. Soc. Am*., **95**, 896-903, 2005.

Hauksson, E., W. Yang and P. M. Shearer (2012). Waveform relocated earthquake catalog for southern California (1981 to June 2011), *Bull. Seismol. Soc. Am.*, **102**, 2239–2244, doi: 10.1785/0120120010.

Hardebeck, J.L. and Michael, A.J., (2006). Damped regional-scale stress inversions: methodology and examples for southern California and the Coalinga aftershock sequence, *J. Geophys. Res.,* 111, B11310.

Hardebeck, J. L., and P. M. Shearer (2002), A new method for determining first-motion focal mechanisms, Bull. Seismol. Soc. Am., 92, 2264–2276.

Hunter, L.E., Howle, J.F., Rose, R.S., and Bawden, G.W., (2011), LiDAR-assisted identification of an active fault near Truckee, California: Bulletin of the Seismological Society of America, v. 101, p. 1162-1181.

Ichinose, G. A., K. D. Smith, and J. G. Anderson (1998), Moment tensor solutions of the 1994 to 1996 Double Spring Flat, Nevada, earthquake sequence and implications for local tectonic models, Bull. Seismol. Soc. Am., 88(6), 1363–1378.

Ichinose, G.A., Roman-Nieves, and Kraft, G. (2014). Moment Tensor Inversion Toolkit (MTINV) Documentation, Manual and Tutorial, Version 3.0.3 Release Date: March 7, 2014.

Klein, F. W. (2002), User's Guide to HYPOINVERSE-2000, a Fortran Program to Solve for Earthquake Locations and Magnitudes Open File Report 02-171 Version 1.0.

Lin, G., P. M. Shearer and E. Hauksson (2007). Applying a three-dimensional velocity model, waveform cross correlation, and cluster analysis to locate southern California seismicity from 1981 to 2005, *J. Geophys. Res.*, **112**, B12309, doi: 10.1029/2007JB004986.

Reeves, D.M., Smith, K.D., Rarahar, R., Collins, C., HeintZ, K.M. (2016). Investigating the Influence of Regional Stress of Fault and Fracture Permeability at Pahute Mesa, Nevada National Security Site, special study prepared for the Nevada Site Office, National Nuclear Security Administration, U.S. Department of Energy Las Vegas, Nevada, pp. 107.

Shearer, P. M., G. A. Prieto, and E. Hauksson, (2006). Comprehensive analysis of earthquake source spectra in southern California, *J. Geophys. Res.***, 111**, B06303, doi:10.1029/2005JB003979.

Trugman, D. T. and Shearer, P.M. (2017a). GrowClust: A Hierarchical Clustering Algorithm for Relative Earthquake Relocation, with Application to the Spanish Springs and Sheldon, Nevada, Earthquake Sequences, *Seism. Res. Lett*., 88, February 2017.

Trugman, D. T. and P. M. Shearer (2017b), Application of an improved spectral decomposition method to examine earthquake source scaling in southern California, *J. of Geophys. Res, Solid Earth*, 122(4), doi:10.1002/2017JB013971.

van Wormer, J.D., and A.S. Ryall, Sierra Nevada-Great Basin boundary zone: Earthquake hazard related to structure, active tectonic processes, and anomalous patterns of earthquake occurrence, *Bull. Seismol. Soc. Am.*, **70**, 1557-1572, 1980.

Waldhauser, F. (2001). HypoDD: A computer program to compute double-difference earthquake locations, USGS Open File Rep., 01-113.

Zaliapin, I., and Y. Ben-Zion (2013a), Earthquake clusters in southern California I: Identification and stability, J. Geophys. Res. Solid Earth, 118, 2847–2864, doi:10.1002/jgrb.50179.

Zaliapin, I., and Y. Ben-Zion (2013b), Earthquake clusters in southern California II: Classification and relation to physical properties of the crust, J. Geophys. Res. Solid Earth, 118, 2865–2877, doi:10.1002/jgrb.50178.